

Aino Manninen

# **Evaluation of the effects of design choices on surface mounted permanent magnet machines using an analytical dimensioning tool**

**Sähkötekniikan korkeakoulu**

Diplomityö, joka on jätetty opinnäytteenä tarkastettavaksi  
diplomi-insinöörin tutkintoa varten Espoossa 25.5.2012.

Työn valvoja:

Prof. Antero Arkkio

Työn ohjaajat:

TkT Jenni Pippuri, tutk. prof. Kari Tammi



**Aalto-yliopisto**

Sähkötekniikan  
korkeakoulu

AALTO-YLIOPISTO SÄHKÖTEKNIIKAN KORKEAKOULU	DIPLOMITYÖN TIIVISTELMÄ
Tekijä: Aino Manninen	
Työn nimi: Kestomagnetoidun tahtikoneen suunnitteluparametrien vaikutuksen arviointi analyyttisen mitoitustyökalun avulla	
Päivämäärä: 25.5.2012	Kieli: englanti
Sivumäärä: 76 + 5	
Sähkötekniikan laitos	
Professori: Sähkömekaniikka	Koodi: S-17
Valvoja: prof. Antero Arkkio	
Ohjaajat: TkT Jenni Pippuri, tutk. prof. Kari Tammi	
<p>Tämä diplomityö käsittelee kestopagnetoidun tahtikoneen suunnitteluparametrien kuten esimerkiksi napapariluvun tai ilmavälivuontiheyden vaikutusta koneen ominaisuuksiin. Työssä toteutettiin analyyttisiin laskentakaavoihin perustuva mitoitustyökalu pintamagneetikoneelle, jonka staattorissa on yksikerroskäämitys. Tämän avulla pyrittiin selvittämään, miten eri suunnitteluparametrien valinta vaikuttaa koneen hyötysuhteeseen, tehokertoimeen, kokoon sekä kestopagneettimateriaalin määrään. Erityisesti pyrittiin selvittämään, miten koneesta voitaisiin saada mahdollisimman kompakti.</p> <p>Toteutettu mitoitustyökalu verifioitiin vertaamalla sen antamia tuloksia elementtimenetelmällä laskettuihin tuloksiin. Esimerkkinä työkalua testattiin kuvitteellisen 22 kW teollisuuspumpun suunnittelemiseen. Suunnitteluparametrien vaikutuksen selvittämiseksi työkalulla laskettiin joukko erilaisia mitoituksia valitulle koneelle. Havaittiin, että koneesta saadaan kevyempi kasvattamalla napaparilukua, virran tiheyttä staattorikäämityksessä sekä magneettivuon tiheyttä staattorissa. Tällöin haittapuolena oli hyötysuhteen huononeminen.</p>	
Avainsanat: kestopagnetoitu tahtikone - suunnittelu - mitoitustyökalu	



## **Foreword**

This Master's Thesis was carried out at Electrical Product Concepts Team at VTT in Espoo. I want to thank my instructors D.Sc. (Tech.) Jenni Pippuri and Res. Prof. Kari Tammi and my supervisor Prof. Antero Arkkio. I also want to express my thanks to D.Sc. (Tech.) Janne Keränen for providing validation data for my dimensioning tool.

Otaniemi, 25.5.2012

Aino Manninen

# Contents

Foreword .....	4
Nomenclature .....	7
Abbreviations.....	7
Symbols .....	7
1 Introduction .....	11
1.1 Objective .....	11
1.2 Permanent magnet synchronous machines.....	12
2 Methods.....	15
2.1 Design procedure.....	15
2.1.1 Initial parameters .....	15
2.1.2 Mechanical dimensions .....	16
2.1.3 Winding.....	18
2.1.4 Permanent magnets .....	20
2.1.5 Calculating the flux and the flux density.....	20
2.1.6 Slot dimensions.....	22
2.1.7 Inductances .....	25
2.1.8 Torque, resistances and power losses.....	27
2.1.9 Heat transfer .....	31
2.1.10 Thermal analysis of the PMSM .....	34
2.2 MATLAB implementation.....	40
2.3 Operation profile.....	44
3 Results .....	47
3.1 Validation of the dimensioning tool .....	47
3.2 Description of the calculation process of results .....	51
3.3 Machine properties explored.....	53
3.4 Effects of the initial design parameters.....	54
3.4.1 Pole pair number .....	54
3.4.2 Machine length to air gap diameter ratio.....	58
3.4.3 Air gap.....	60
3.4.4 Relative magnet width.....	62
3.4.5 Current density.....	64
3.4.6 Air gap flux density.....	67

4	Discussion .....	70
4.1	Conclusions .....	70
4.2	Further work.....	73
	References .....	75
	Appendix 1: Explanation of the d- and q-axis and the inductances .....	77
	Appendix 2: Dimensions and other parameters for validated models .....	79

# Nomenclature

## Abbreviations

AC	Alternating current
AlNiCo	Aluminium-nickel-cobalt
DC	Direct current
EMF	Electromotive force
FEM	Finite element method
NdFeB	Neodymium-iron-boron
PMSM	Permanent magnet synchronous machine

## Symbols

### Latin

$A$	armature linear current density
$a$	number of parallel paths
$\alpha_1, \alpha_2, \alpha_3$	empirical heat transfer constants
$\hat{B}$	peak magnetic flux density
$b$	width
$C$	machine constant related to apparent power
$c$	coefficient
$\cos \varphi$	power factor
$D$	diameter
$E_{PM}$	back induced EMF
$F$	bearing load
$f$	frequency
$f_r$	iron space factor
$G_{th}$	thermal conductance
$\mathbf{G}_{th}$	thermal conductance matrix
$\hat{H}$	magnetic field strength
$h$	height
$I$	current
$J$	current density
$k_1, k_2, k_3$	empirical coefficients
$k_{cond}$	number of parallel conductors in one slot
$k_{Cu}$	copper space factor
$k_{Fe}$	saturation factor

$k_{Fe,t}$	coefficient for iron losses, teeth
$k_{Fe,y}$	coefficient for iron losses, yoke
$k_{dv}$	distribution factor
$k_{pv}$	pitch factor
$k_R$	resistance factor
$k_{wv}$	winding factor
$l$	length, thickness
$l'$	effective machine length
$L$	inductance
$l_{av}$	average length of a coil turn
$l_c$	total length of a conductor in a coil
$l_{cond}$	length of one coil turn
$l_m$	thickness of permanent magnets
$l_{m,eff}$	effective thickness of permanent magnets
$l_p$	width of permanent magnets
$m$	mass, number of phases
$N$	number of turns in a winding
$Nu$	Nusselt number
$N_c$	number of coil turns in a slot
$N_{ph}$	number of coil turns in a phase
$n$	rotating speed
$n_{syn}$	synchronous speed
$n_v$	number of ventilation ducts
$m$	number of phases
$P$	output power
$P_{Br}$	mechanical losses
$P_{Cu}$	resistive losses
$P_{Fe}$	iron losses
$P_{el}$	electrical power
$P_{mec}$	mechanical power
$P_{Str}$	additional losses
$\mathbf{P}$	heat flow source vector
$p$	pole pair number
$p_{10}$	coefficient
$Q$	number of slots
$q$	number of slots per pole per phase
$R$	resistance, reluctance, thermal resistance
$r$	radius
$S$	area [m <sup>2</sup> ], apparent power
$T$	torque, temperature
$Ta$	Taylor number
$Ta_m$	modified Taylor number
$T_{rel}$	relative torque
$T_1$	fundamental torque
$t$	time
$U_{ph}$	stator phase voltage

$v$	velocity
$W$	coil span (width)
$z$	tooth width
$z_Q$	number of conductors in a slot

### Greek

$\alpha_{PM}$	relative magnet width
$\alpha_{th}$	heat transfer coefficient
$\alpha_u$	slot angle
$\gamma$	coefficient
$\delta$	air-gap
$\delta_a$	load angle
$\varepsilon_{thr}$	relative emissivity
$\eta$	efficiency
$\Theta$	temperature difference
$\vec{\Theta}$	temperature vector
$\lambda$	thermal conductivity [W/K m]
$\mu_{PM}$	relative permeability of permanent magnets
$\mu_0$	permeability of vacuum, constant $4\pi \times 10^{-7}$ [V s/A m]
$\nu$	ordinal of harmonic, magnetic voltage
$\nu_A$	kinematic viscosity of air
$\chi$	the ratio of the equivalent machine length to the air-gap diameter
$\pi$	constant, 3.14...
$\rho$	mass density
$\sigma$	electrical conductivity
$\sigma_{SB}$	Stefan-Boltzmann constant, $5.67 \cdot 10^{-8}$ W/m <sup>2</sup> K <sup>4</sup>
$\tau_p$	pole pitch
$\tau_u$	slot pitch
$\tau_y$	length of the pole pitch in the middle of the yoke
$\Phi$	magnetic flux, heat flow rate
$\Omega$	mechanical angular speed
$\omega$	angular frequency

### Subscripts

0	shortest
1, 2, 3, ...	numbers, indexes
AC	alternating current
Al	aluminium
av	average
b	bearing
bb	from bearing to bearing
c	coil
cond	subconductor
cr	contact between the rotor yoke and the shaft
cy	contact between yoke and frame
d	d-axis

DC	direct current
eff	effective
es	end shield
Fe	iron
fin	cooling fin
fr	frame
i	index
if	internal frame
ins	insulation
Ir	insulation
m	magnets
md	magnetizing inductance, d-axis
mec	mechanical
mq	magnetizing inductance, q-axis
n	nominal
p	width of permanent magnets
ph	phase
PM	permanent magnets
q	q-axis
r	rotor
s	slot, stator
se	stator outer
sh	shaft
sl	retaining sleeve
sq	skew
T	temperature
th	thermal
tt	tooth tip
u	slot
v	ventilation duct
ve	equivalent ventilation duct
w	endwinding
wp	working period
x,y	per unit length
x0, y0	slot material, effective rectangular slot
y	yoke
yr	rotor yoke
z	teeth
$\delta$	air-gap
$\sigma$	leakage

# 1 Introduction

Permanent magnet synchronous machines (PMSMs) were first introduced in the 1930's when the AlNiCo magnet material was discovered. However, at that time the performance of the magnet material was not sufficient and variable frequency power sources did not exist, which made the use of the PMSM very limited. Nowadays the permanent magnet materials are better, particularly after the neodymium-iron-boron (NdFeB) -magnets were discovered in 1983. It is also possible to use frequency converters to control the PMSMs. These improvements have made permanent magnet synchronous machines more popular. [1]

The permanent magnet synchronous machine has several advantages such as a maintenance-free operation, high controllability, robustness against the environment, high power factor and high efficiency. The environmental problems have caused a need to save energy. This means a growing demand for highly efficient electrical machines. The development of high performance magnet material in addition to environmental issues has expanded the field of applications for PMSM. [1] The PMSMs are widely used for example in hybrid vehicles.

In order to be able to produce efficient and compact PMSMs, the design criteria have to be known. There are certain properties that are interesting from the energy conservation point of view, for example efficiency, power density and power factor. Also the material costs have to be taken into account. For example the permanent magnet materials are usually rather expensive. Compared to the price of copper, the price of NdFeB-magnet material is about 11 times higher [2], [3]. These properties can be affected by changing several different design parameters. The parameters include pole pair number, the size of permanent magnets, the type of winding, etc.

The design of an electrical machine is a rather complicated task that contains several steps. During these steps, some of the qualities of the machine become fixed by means of empirical equations. This makes the optimization of the machine design a rather difficult task. In order to be able to define an optimal solution for certain initial conditions, it is important to know how the different design parameters affect the final outcome. For example the pole pair number might have a certain effect on the size of the machine or the stator current density might affect the efficiency. Because there are several parameters that have to be optimized, the final solution is always a compromise between different criteria.

## 1.1 Objective

The objective of this Master's Thesis is to investigate the effect of the design parameters and find possible contradictions between different parameters. These contradictions could then be used for optimization. One objective is to study how to design more compact machines. To study the design parameters a dimensioning tool

is implemented using the MATLAB software of MathWorks [4]. The tool is based on analytical design equations of electrical machines. The investigation is restricted to surface mounted permanent magnet synchronous machines because of their simple geometry. In addition, only single layer integer slot stator windings are considered at this stage. Later it would be possible to further implement the dimensioning tool to work also with for example other rotor or winding topologies.

The first chapter describes the structure and purpose of this thesis and introduces permanent magnet synchronous machines. The second chapter discusses the design process of PMSMs. Also the implemented design tool is presented. The analysis of the effects of different design parameters is presented in Chapter 3 and the conclusions drawn from this analysis are discussed in Chapter 4.

## 1.2 Permanent magnet synchronous machines

A synchronous machine is an electrical machine that operates at synchronous speed meaning the speed at which the magnetic field rotates. The synchronous speed depends on the frequency of the applied voltage and the number of poles in the machine. The permanent magnet machines can be operated at unity power factor and can therefore provide better efficiency than for example induction machines. The PMSM has also high efficiency, high torque density and good heat dissipation. It is possible to make the torque smooth and the pull-out torque high. On the other hand, the PMSMs are expensive, because of the high prices of the magnet materials. Because the magnetization is constant, the field weakening properties are poor compared to ordinary synchronous machines. [5]

The basic components are stator and rotor. The stator is also the armature of the synchronous machine. The stator core is made of thin laminations of highly permeable steel. The stator core is placed inside an aluminium frame. The main purpose of the frame is to provide mechanical support for the synchronous machine. Inside the stator core there is a plurality of slots as can be seen from Figure 1. The coils that form a polyphase winding, are arranged symmetrically in these slots. [6]

According to [6] the synchronous machines usually operate at three phase power and the armature winding is thus made of three separate windings. The three phase windings may be connected to either star (Y) or delta ( $\Delta$ ) connection. The winding can be a single layer or a double layer winding. In a double layer winding there are two coil sides in a slot whereas in a single layer winding there is only one. The winding is an integer slot winding if the number of slots per pole per phase is an integer. Otherwise the winding is called a fractional slot winding.

The armature winding of the synchronous machine produces a revolving magnetic field. When the north pole of the field is just above the south pole of the rotor, the force attraction between the two poles starts to move the rotor. Because the rotor is

heavy, it takes time before it can start moving, and by the time it starts to move, the revolving field has changed its polarity. Now there are poles with alike polarity close to each other and the repulsive force tries to move the rotor to the other direction. This means that the synchronous machine is typically not self-starting without a frequency converter. [6]

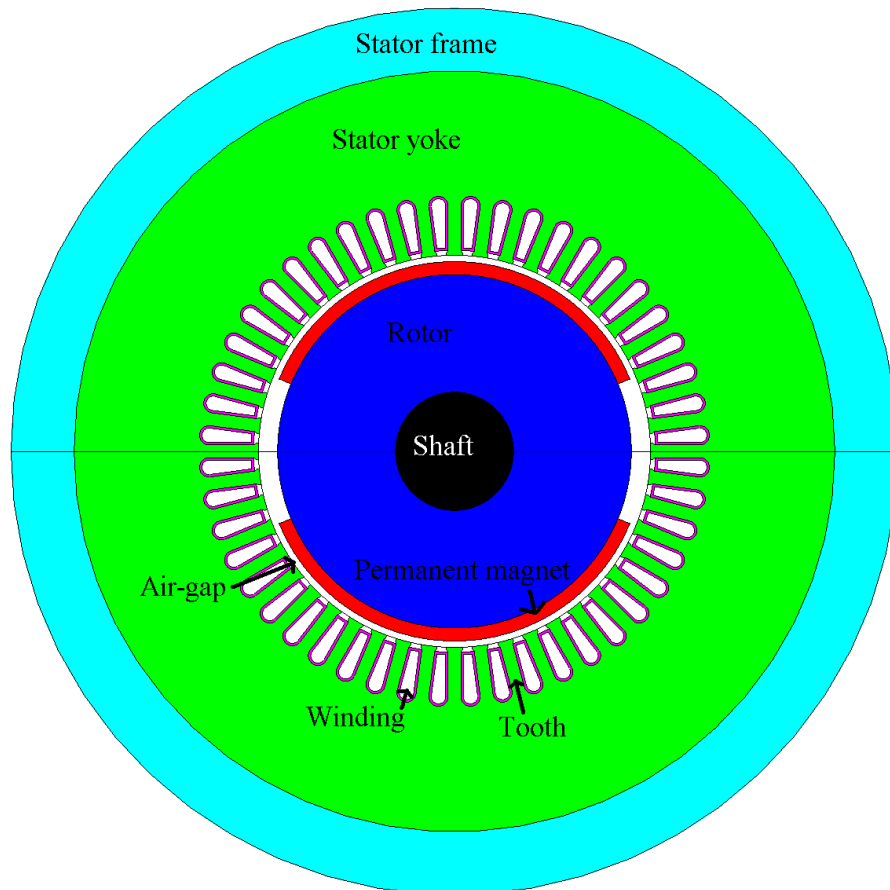


**Figure 1. Structure of a two-pole surface-mounted permanent magnet synchronous machine.**

The rotor is rotated at synchronous speed. In permanent magnet synchronous machines the main magnetic field is created by permanent magnets that are mounted to the rotor. The rotor core is either solid iron, or made of laminations. The permanent magnets can be mounted to the core in several ways. In surface permanent magnet machines, the magnets are mounted on the surface of the outer periphery of rotor laminations. Since the relative permeability of the magnet material is close to one, this kind of structure has a large effective air gap, and the d-axis inductance is thus low. [5] (See Appendix 1 for the definitions of the d- and q-axis.)

Because the permanent magnets produce a constant flux in the air gap, the field weakening properties of a surface magnet machine are poor. Most of the current would go to demagnetization, and very little current would be left to produce torque. If high operation speed is needed, the nominal rotation speed of the surface mounted PMSM should thus be close to the needed operation speed. The surface magnet construction might also need a fibre glass band to make the construction mechanically robust enough. One drawback is also that the frequency converter produces higher order harmonics. An advantage of the surface magnet construction is that the leakage flux is low, because there is no ferromagnetic path for the flux at the edges of the magnet. Reduced quadrature axis inductance decreases the armature reaction which leads into a smaller pole angle and higher torque. For this reason, less permanent magnet material is usually needed for the surface magnet machine than for the interior magnet machine. [5] High speed machines are typically surface mounted PMSMs.

The magnets can be also buried in the rotor. There are a lot of possibilities to place the magnets in the rotor. A common geometry is presented in Figure 2, where the magnets are in V-shape. This kind of construction is typically used in industry. A drawback of this kind of construction is that it requires usually more magnet material than the surface mounted magnets. [5] The V-shaped interior permanent magnet construction is also less robust mechanically, since there are only small iron bridges to hold the magnets. On the other hand, it is possible to use rectangular magnets which are easier to produce than the curved ones.

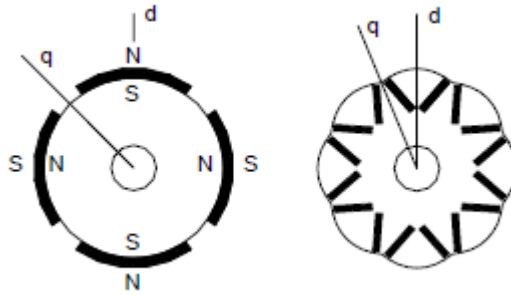


**Figure 2. Two different permanent magnet rotor structures: surface mounted magnets (left) and interior magnets (right). [7]**

## 2 Methods

### 2.1 Design procedure

#### 2.1.1 Initial parameters

Usually the electrical machine is designed for given initial conditions. The system for which the machine is intended defines the requirements concerning shaft power, supply voltage and speed.

Besides the above ones, there are several other initial parameters that also affect the machine design process. The current density in the stator winding and the magnetic flux density in the air-gap can be estimated relatively easily because there are certain restrictions to both of them. If the magnetic flux density is too low, the iron core is not utilized well. On the other hand when the flux density is too large, the iron will saturate. If the current density is too high the conductors will overheat, which may damage the insulations. According to [8] the current density in a stator winding of a PMSM varies between 4-6.5 A/mm<sup>2</sup> and the air gap flux density of a non-salient pole synchronous machine varies between 0.8-1.05 T.

Initial estimates for efficiency and power factor are chosen. An initial value for the needed electrical power  $P_{el}$  is calculated using the estimated efficiency  $\eta$

$$P_{el} = \frac{P_{mec}}{\eta}, \quad (1)$$

where  $P_{mec}$  is the mechanical power. The linear current density is also estimated. In order to find the linear current density, the machine constant has to be determined. The machine constant expresses the magnitude of the internal apparent power or mechanical power given by the rotor volume of the machine. Because the machine constant can be calculated using either apparent power or mechanical power, it means that there are actually two slightly different machine constants. Here the mechanical machine constant  $C_{mec}$  is used to determine the mechanical dimensions and the apparent machine constant  $C$  is used to obtain the desired linear current density in the stator.

There is a relation between the mechanical machine constant and the apparent machine constant. According to [8] the apparent power is

$$S = CD^2l'n_{syn}, \quad (2)$$

where  $n_{syn}$  is the synchronous speed  $l'$  is the effective length of the machine and  $D$  is the air gap diameter i.e. stator inner diameter. The mechanical power is

$$P_{\text{mec}} = \eta \cos \varphi \frac{U_{\text{ph}}}{E_{\text{PM}}} S = C_{\text{mec}} D^2 l' n_{\text{syn}}, \quad (3)$$

where  $\cos \varphi$  is the power factor and  $E_{\text{PM}}$  is the back induced electromotive force (back-EMF). By substituting  $S$  in Equation (3) with Equation (2), we get

$$\eta \cos \varphi \frac{U_{\text{ph}}}{E_{\text{PM}}} C D^2 l' n_{\text{syn}} = C_{\text{mec}} D^2 l' n_{\text{syn}}. \quad (4)$$

Now a relation between the apparent and the mechanical machine constants is obtained

$$C = \frac{C_{\text{mec}}}{\cos \varphi \eta U_{\text{ph}} / E_{\text{PM}}}, \quad (5)$$

where  $U_{\text{ph}}$  is the phase voltage. For rotating electrical machines the apparent machine constant can be written also

$$C = \frac{\pi^2}{\sqrt{2}} k_{\text{w1}} A \hat{B}_{\delta}, \quad (6)$$

where  $A$  is the linear current density in the stator,  $\hat{B}_{\delta}$  is the peak flux density in the air gap and  $k_{\text{w1}}$  is a winding factor which depends on the winding arrangement. Here Equation (5) is used to solve the initial value of the linear current density. At this point of the design process, the actual value of the winding factor is not yet known, but since it does not vary very much, it can be guessed to be for example 0.92 just to obtain an initial guess for the linear current density.

The pole pair number  $p$  depends on the speed  $n$  and the frequency  $f$

$$n = \frac{f}{p} \Rightarrow p = \frac{f}{n}, \quad (7)$$

If the machine is supplied from a frequency converter, which normally is the case with PMSMs, the machine properties can be affected by choosing a suitable number of poles.

### 2.1.2 Mechanical dimensions

The most interesting mechanical dimensions are the actual length of the machine and the stator outer diameter, because these two roughly determine the machine size. The larger these values are the larger the machine volume and usually the heavier the mass usually are. To be able to construct the mechanical parts of the machine, also the detailed dimensions for the stator and rotor are needed.

In the case of the stator, the inner and outer diameters of the stator core, the height of the yoke and the teeth, the width of the teeth, the slot dimensions and the number of slots need to be found. The slot dimensions depend on the chosen slot shape. The rotor dimensions in this case are the rotor inner and outer diameter.

There are two mechanical dimensions that are considered as free design parameters, namely air gap length and ratio of machine length to stator inner diameter. Pyrhönen et. al. [8] give also equations to get typical values of these parameters.

The ratio of the effective machine length to the air-gap diameter is

$$\chi = \frac{l'}{D}. \quad (8)$$

where  $l'$  is the effective machine length and  $D$  is the air-gap diameter.

For synchronous machines this value is typically [8]

$$\chi \approx \frac{\pi}{4p} \sqrt{p}, \quad p > 1 \quad (9)$$

$$\chi = 1 \dots 3, \quad p = 1 \quad (10)$$

The mechanical machine constant  $C_{\text{mec}}$  can be obtained from a figure given by [8] p. 289, when  $P_{\text{mec}}/2p$  is known. The mechanical power  $P_{\text{mec}}$  is

$$P_{\text{mec}} = C_{\text{mec}} D^2 l' n = C_{\text{mec}} D^3 \chi n. \quad (11)$$

Now it is possible to solve the air-gap diameter from Equation (11)

$$D = \sqrt[3]{\frac{P_{\text{mec}}}{C_{\text{mec}} \chi n}}. \quad (12)$$

and the effective length  $l' = \chi D$  from Equation (8).

The stator dimensions can be defined when the machine constant is known. These are stator length, the inner and outer diameters of the stator and number of slots in the stator and the length of the air-gap.

The air-gap of a synchronous machine can be estimated by equation

$$\delta \geq \frac{1}{2} \alpha_{\text{SM}} \mu_0 \tau_p \frac{A}{\hat{B}_\delta} = \gamma \tau_p \frac{A}{\hat{B}_\delta}, \quad (13)$$

where  $\gamma$  is a coefficient. For example Pyrhönen et. al. [8] provide a table for choosing a suitable value for  $\gamma$ .  $A$  is the armature linear current density,  $\hat{B}_\delta$  is the

peak air-gap flux density and  $\tau_p$  is the pole pitch. In PMSMs the air-gap length is determined by mechanical constraints. It is similar to the values encountered with asynchronous machines, and can therefore be calculated using same equations [8]:

$$\delta = \frac{0.2 + 0.01P^{0.4}}{1000} \text{ m}, \quad p = 1 \quad (14)$$

$$\delta = \frac{0.18 + 0.006P^{0.4}}{1000} \text{ m}, \quad p > 1 \quad (15)$$

Now also the rotor core diameter  $D_r$  can be calculated from equation

$$D = D_r + 2\delta + 2l_m. \quad (16)$$

where  $\delta$  is the air gap and  $l_m$  is the thickness of the permanent magnets.

The effective machine length differs from the real machine length for two reasons. First, there are ventilation ducts in the machine that make the machine real length larger than the effective. The effect of the air-gap has to be taken into account too. The effective length of the machine is

$$l' \approx l + 2\delta - n_v b_{ve}, \quad (17)$$

which means that the actual length is approximately

$$l \approx l' - 2\delta + n_v b_{ve}, \quad (18)$$

where  $n_v$  is number of ventilation ducts and  $b_{ve}$  is the effective width of the ventilation ducts.

### 2.1.3 Winding

The next task is to design a suitable winding for the machine. Only single layer, integer slot windings are considered here. There is only one coil side in each slot and the number of slots per pole per phase  $q$  is an integer. The two main tasks of the design procedure are to define a suitable winding and to find suitable dimensions for the permanent magnets. These two properties are connected to each other via the back induced EMF

$$E_{PM} = \frac{2\pi f k_{w1} N_{ph} \hat{\Phi}_{\delta,PM}}{\sqrt{2}}. \quad (19)$$

It can be seen from Equation (19) that the back-EMF depends on the number of coil turns in a phase  $N_{ph}$ , the maximum magnetic flux in the air-gap  $\hat{\Phi}_{\delta,PM}$ , the winding factor  $k_{w1}$  and the supply frequency  $f$ . The winding factor and the number of coil

turns in a phase depend on the winding whereas the air-gap flux is generated by the permanent magnets. The back-EMF affects the power factor of the machine. If the back-EMF is close to the phase voltage, the power factor should be close to one. This means that when the winding is defined, the permanent magnet dimensions can be solved using Equation (19). Designing the winding includes defining the number of slots per pole per phase, number of conductors in a slot and number of coil turns in a phase. The winding is chosen so that the obtained linear current density is close to the approximated one. The linear current density depends of the number of coil turns and the stator inner diameter

$$A = \frac{2I_s N_{ph} m}{\pi D}, \quad (20)$$

where  $I_s$  is the stator current and  $m$  is the number of phases. When the winding is chosen, the winding factor is calculated. The winding factor  $k_{wv}$  of a harmonic  $v$  is

$$k_{wv} = k_{pv} k_{dv} \quad (21)$$

where the pitch factor is

$$k_{pv} = \sin\left(v \frac{W \pi}{\tau_p 2}\right) \quad (22)$$

and the distribution factor is

$$k_{dv} = \frac{\sin\left(\frac{vq\alpha_u}{2}\right)}{q \sin\left(\frac{v\alpha_u}{2}\right)}, \quad (23)$$

where

$$\alpha_u = \frac{p2\pi}{Q} \quad (24)$$

is the slot pitch angle which is measured in electrical degrees,  $q$  is the number of slots per pole per phase, and  $Q$  is the number of slots.  $v$  can be  $v = +1 \pm 2cm$ , where  $c$  is any positive integer or zero and  $m$  is the number of phases. For one layer winding,  $W = \tau_p$ , which makes the pitch factor

$$k_{pv} = \sin\left(\frac{v\pi}{2}\right). \quad (25)$$

The number of the stator slots defines the slot pitch

$$\tau_u = \frac{\pi D}{Q}. \quad (26)$$

The maximum number of slots is reduced by the length of the stator inner periphery. Typical slot pitches are given in [8]. For small PMSMs this is 7-45 mm and for large PMSMs 14-75 mm. The number of stator slots can also be determined by defining the number of slots per pole per phase  $q$ .

$$q = \frac{Q}{2pm}. \quad (27)$$

#### 2.1.4 Permanent magnets

Next, the permanent magnets will be designed. The material of the magnets is chosen and the dimensions are defined. The most important characteristics for the permanent magnet material are the remanence flux density  $B_r$ , coercive field strength  $H_c$ , the second quarter of the hysteresis loop, the energy product, temperature coefficients of the remanence flux density and coercive field strength, resistivity, and mechanical and chemical characteristics. [8]

Two common permanent magnet rotor structures are a surface permanent magnet rotor and an interior permanent magnet rotor, where the magnets are in a V-shape. These structures are presented in Figure 2. Since the geometry and calculations are simpler with surface magnets than with interior magnets, the surface magnet rotor was chosen for this study.

The surface magnet dimensions include the thickness of the permanent magnets  $l_m$  and the width of the magnets  $l_p$ . The width  $l_p$  has to be smaller than the pole pitch  $\tau_p$ . Usually the magnet width is about 0.8 – 0.85 times the pole pitch. [9] The magnet thickness should be as small as possible to keep the amount of permanent magnet material that is needed low. However, the magnets have to be thick enough to produce the required air-gap magnetic flux. The magnet thickness can be chosen iteratively when a suitable width has been chosen. The thickness is optimal when the back-EMF calculated by Equation (19) equals approximately the phase voltage. It is possible to allow the back-EMF to be smaller than the phase voltage, but that will also lead to a smaller power factor.

#### 2.1.5 Calculating the flux and the flux density

Now the magnetic flux and flux density in the air-gap are calculated. For this purpose, a reluctance network model of the machine is employed. In Figure 3 a reluctance network for a surface magnet PMSM is presented.  $R_{PM}$  is the reluctance of the permanent magnets,  $R_{Fe}$  is the iron reluctance which consists of the stator teeth reluctance  $R_z$  and the stator yoke reluctance  $R_s$ .  $R_{\delta 2}$  is the reluctance of the air-gap between two magnets and  $R_{\delta}$  is the air-gap reluctance in the minimum air-gap between the stator and the magnets.  $\Phi_{PM}$  is the total magnetic flux of the permanent magnets,  $\Phi_{\delta, PM}$  is the air-gap flux and  $\Phi_{\sigma}$  is the leakage flux. [7]

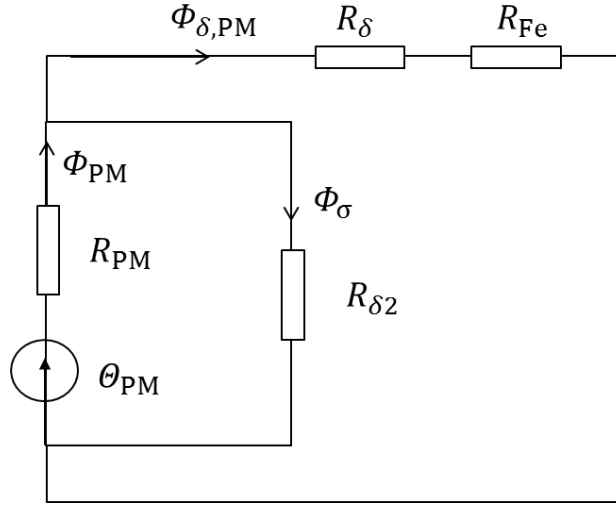


**Figure 3. Reluctance network model for a surface magnet PMSM.**

The equation for the air-gap flux  $\Phi_{\delta,PM}$  can be derived from the reluctance network

$$\Phi_{\delta,PM} = \frac{\theta_{PM}}{R_{PM} + R_{\delta} + R_{Fe}(n) + \frac{R_{PM}}{R_{\delta 2}}(R_{\delta} + R_{Fe}(n))}. \quad (28)$$

The reluctance of the air-gap between the permanent magnets and the stator is

$$R_{\delta} = \frac{\delta_0}{\mu_0 \tau_p l'}. \quad (29)$$

The reluctance of the air-gap between two magnets is

$$R_{\delta 2} = \frac{l_m}{\mu_0 (\tau_p - l_p) l'}. \quad (30)$$

The reluctance of the permanent magnets is

$$R_{PM} = \frac{l_m}{\mu_0 \mu_{PM} l_p l} + \frac{l_t}{\mu_0 l_p l} \quad (31)$$

where  $l_t$  is the thickness of the insulation layer between the rotor and the magnets,  $l_m$  is the thickness of the magnets and  $l_p$  is the magnet width,  $l$  is the actual length of the machine,  $\mu_0$  is the permeability of vacuum and  $\mu_{PM}$  is the relative permeability of the permanent magnets.

Calculation of the magnetic flux is an iterative process. Because the slot dimensions are not known beforehand, it is not possible at the first iteration to calculate the iron reluctance. This problem is solved by calculating an initial guess for the magnetic flux density in the air-gap. This is used to solve the magnetic flux from Equation

(32). Now it is possible to solve the slot dimensions. This is explained more carefully in Section 2.1.6.

The maximal air-gap flux density is

$$\hat{B}_\delta(n) = \frac{\hat{\Phi}_{\delta,PM}(n)}{\alpha_{PM}\tau_p l'} \quad (32)$$

where  $\alpha_{PM}$  is the relative magnet width  $\alpha_{PM} = \frac{l_p}{\tau_p}$ ,  $\tau_p$  is the pole pitch, and  $l'$  is the effective length of the machine. [7]

If the slot dimensions are known, the iron reluctance is relatively simple to calculate. The yoke reluctance is

$$R_{Fey} = \frac{w_y}{\mu_{Fey}\mu_0 l h_y}, \quad (33)$$

where  $w_y$  is the yoke width,  $h_y$  is the yoke height and  $\mu_{Fey}$  is the permeability of iron in the yoke. The reluctance of the teeth is

$$R_{Fet} = \frac{h_z}{\mu_{Fetz}\mu_0 l b_z}, \quad (34)$$

where  $h_z$  is the tooth height,  $b_z$  the tooth width and  $\mu_{Fetz}$  the permeability of iron in the tooth. The total iron reluctance is now

$$R_{Fe} = R_{Fet} + \frac{1}{2} R_{Fey} \quad (35)$$

### 2.1.6 Slot dimensions

When the magnet dimensions and the air-gap flux density are known, the next step is to calculate the dimensions of the stator slots and teeth. Here, the tooth width is chosen to be constant and the slot shape is presented in Figure 4. The needed slot dimensions are the minimum width  $bs1$ , maximum width  $bs2$ , height  $h_z$  and the height of the conductor area  $h4$ . The height  $h_z$  is used for both slot and tooth heights.

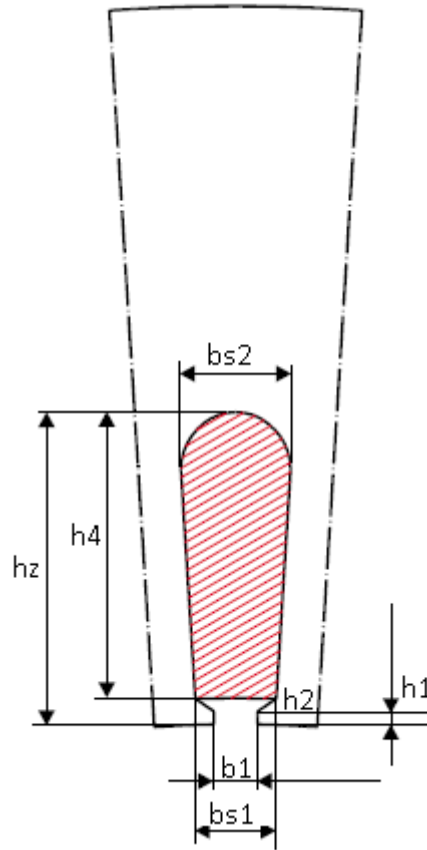


**Figure 4. Stator slot shape.**

At first step, the maximum magnetic flux densities for the teeth and the yoke are selected. According to [8] a maximum value for the tooth flux density  $\hat{B}_z$  is 1.5-2.0 T and for the yoke  $\hat{B}_y$  1.1 – 1.5 T. Because the air-gap flux density distribution is rectangular in the air gap, the flux density in the teeth is

$$\hat{B}_z = \frac{l' \tau_u}{S_z} \hat{B}_\delta \quad (36)$$

above the magnets and zero elsewhere. [7]  $S_z$  denotes the cross-sectional area of a tooth and according to [8] it is

$$S_z = f_r (l - n_v b_v) b_z \quad (37)$$

where  $f_r$  is the filling factor for the iron laminates,  $n_v$  is the number of ventilating ducts and  $b_v$  is the width of the a duct. The maximum magnetic flux passing through one slot pitch is

$$\hat{\Phi}_z = l' \tau_u \hat{B}_\delta. \quad (38)$$

When the tooth is not saturated almost all the flux goes through the tooth, which means that the flux density in the tooth is

$$\hat{B}_z = \frac{l' \tau_u}{f_r (l - n_v b_{ve}) b_z} \hat{B}_\delta \quad (39)$$

where  $l' = l - n_v b_{ve} + 2\delta$  and  $f_r$  is the space factor of laminated iron. Typically  $f_r$  varies between 0.9 and 0.97. The tooth width  $b_z$  can be solved from Equation (39) when the maximal value of the magnetic flux density in a tooth is defined. The slot width is

$$b_s = \tau_u - b_z \quad (40)$$

where  $\tau_u$  is the stator slot pitch.

The length of the stator slot can be determined when the slot area and width are known. In order to calculate the slot area  $S_u$  the stator current  $I_s$  has to be defined first

$$I_s = \frac{P}{m\eta U_{ph} \cos \varphi}. \quad (41)$$

Now the area of conductors is

$$S_c = \frac{I_s}{aJ_s} \quad (42)$$

and the slot area is

$$S_u = \frac{z_Q S_c}{k_{Cu}}. \quad (43)$$

in which  $J_s$  is the current density in the conductors. It is a design parameter that has to be chosen in the beginning of machine design. Furthermore, the  $z_Q$  denotes the number of conductors in a slot,  $S_c$  the area of a conductor and  $k_{Cu}$  the space factor of a slot. The space factor  $k_{Cu}$  depends of the winding material, the voltage level and the winding type. For low-voltage machines, typical values are  $k_{Cu} \in (0.5, 0.6)$  and for high-voltage machines  $k_{Cu} \in (0.3, 0.45)$ , the lower value being for round wires and the upper value for rectangular wires. The number of conductors in a slot  $z_Q$  is defined as

$$z_Q = \frac{2am}{Q} N_{ph}. \quad (44)$$

When the slot area and the minimum slot width are known, the other dimensions can be calculated.

$S_u$  is the total area of the slot. The area that is left between the tooth tips is not taken into account, because there are no conductors in that area. The slot area can be

divided into two parts: a half circle and a trapezium. Now the equation for the area is obtained from geometry

$$S_u = \frac{1}{2}(b_{s1} + b_{s2})h_{tr} + \frac{\pi \left(\frac{b_{s2}}{2}\right)^2}{2}, \quad (45)$$

where  $h_{tr}$  is the height of the trapezium and the other dimensions are as presented in Figure 4. On the other hand the pole pitch reduced to the widest point of the slot is

$$b_{s2} + b_z = \frac{(D + 2h_{tr})\pi}{Q}. \quad (46)$$

Now there are two equations, (45) and (46), from which the two unknown parameters, maximum slot width  $b_{s2}$  and trapezium height  $h_{tr}$ , can be solved. The slot opening  $b_1$  is assumed to be 3/4 of the minimum slot width  $b_{s1}$  and heights  $h_1$  and  $h_2$  are both 1 mm. The slot height satisfies

$$h_z = h_1 + h_2 + h_4, \quad (47)$$

where height  $h_4$  is given as

$$h_4 = h_{tr} + \frac{b_{s2}}{2}. \quad (48)$$

To define the yoke height  $h_y$ , the maximum magnetic flux in the stator yoke has to be calculated. This is rather easy, since in the yoke the maximum flux, namely half of the main flux, flows on the quadrature axis.

$$\hat{B}_y = \frac{\hat{\Phi}_{\delta,PM}}{2f_r(l - n_v b_v)h_y} \Rightarrow h_y = \frac{\hat{\Phi}_{\delta,PM}}{2f_r(l - n_v b_v)\hat{B}_y}. \quad (49)$$

By choosing a maximum allowed value for the flux density in the yoke, the yoke height can now be obtained. The stator outer diameter is

$$D_{se} = D + 2h_z + 2h_y. \quad (50)$$

### 2.1.7 Inductances

When the winding arrangement and the dimensions have been defined, the inductances can be calculated. According to [7] the magnetizing inductance of the direct axis is

$$L_{md} = \frac{m}{2} \frac{4}{\pi} \alpha_i \mu_0 \frac{1}{2p} \frac{\tau_p}{\delta_{deff}} l' (k_{w1} N_{ph})^2 \quad (51)$$

where  $\delta_{\text{deff}}$  is the effective length of the air-gap that depends on the real air-gap length  $\delta_0$ , the thickness of the permanent magnets  $l_m$  and the effect of the saturated iron. In PMSMs, the effective air-gap is obtained as [8]

$$\delta_{\text{deff}} = k_C \delta + l_m / \mu_{\text{PM}} \quad (52)$$

The magnetization inductance of the quadrature axis is similar to the d-axis magnetisation inductance, and the effective air gap  $\delta_{\text{qeff}}$  can be calculated using Equation (52).

$$L_{\text{mq}} = \frac{m}{2} \frac{4}{\pi} \alpha_i \mu_0 \frac{1}{2p} \frac{\tau_p}{\delta_{\text{qeff}}} l' (k_{w1} N_{\text{ph}})^2. \quad (53)$$

The synchronous inductances  $L_d$  and  $L_q$  consist of the magnetizing inductances and leakage inductances

$$L_d = L_{\text{md}} + L_\sigma \quad (54)$$

$$L_q = L_{\text{mq}} + L_\sigma. \quad (55)$$

For more information about the inductances, see Appendix 1. The leakage inductances are assumed to be equal for direct and quadrature axis. The leakage inductance consists of air-gap leakage inductance  $L_\delta$ , slot leakage inductance  $L_u$ , tooth tip leakage inductance  $L_{\text{tt}}$ , end winding leakage inductance  $L_w$  and skew leakage inductance  $L_{\text{sq}}$ .

$$L_\sigma = L_\delta + L_u + L_{\text{tt}} + L_w + L_{\text{sq}}. \quad (56)$$

The air-gap leakage inductance can be calculated multiplying the magnetizing inductance by a leakage factor  $\sigma_\delta$

$$L_\delta = \sigma_\delta L_m \quad (57)$$

$$\sigma_\delta = \sum_{\substack{v=-\infty \\ v \neq 1}}^{v=\infty} \left( \frac{k_{wv}}{v} \right)^2 \quad (58)$$

To calculate the slot leakage inductance  $L_u$  accurately the slot type and the detailed dimensions have to be known. The slot shape chosen for this study is shown in Figure 4. The slot leakage inductance is

$$L_u = \frac{4m}{Q} \mu_0 l' N^2 \lambda_u \quad (59)$$

where

$$\lambda_u = \frac{h_4}{3b_{s2}} + \frac{h_3}{b_{s2}} + \frac{h_1}{b_1} + \frac{h_2}{b_{s2} - b_1} \ln \frac{b_{s2}}{b_1}. \quad (60)$$

Parameters  $h_n$  and  $b_n$  are heights and widths of different slot parts as presented in Figure 4.

The tooth tip leakage inductance for the whole phase winding is obtained by substituting  $\lambda_{tt}$  instead of  $\lambda_u$  in Equation (59).

$$L_{tt} = \frac{4m}{Q} \mu_0 l' N^2 \lambda_{tt} \quad (61)$$

$$\lambda_{tt} = k_2 \frac{5 \left( \frac{\delta}{b_1} \right)}{5 + 4 \left( \frac{\delta}{b_1} \right)}. \quad (62)$$

The coefficient  $k_2 = 1 - \varepsilon$ , when  $\varepsilon = 1 - \frac{W}{\tau_p}$ .

The end winding inductance is

$$L_w = \frac{4m}{Q} q N^2 \mu_0 l_w \lambda_w \quad (63)$$

where  $l_w$  is the average length of the end winding  $l_w = 2l_{ew} + W_{ew}$  and the product  $l_w \lambda_w$  can be written in the form

$$l_w \lambda_w = 2l_{ew} \lambda_{l_{ew}} + W_{ew} \lambda_W. \quad (64)$$

in which  $l_{ew}$  is the axial length of the end winding measured from the end of the stack,  $W_{ew}$  is the coil span and  $\lambda_{l_{ew}}$  and  $\lambda_W$  are the corresponding permeance factors [8].

### 2.1.8 Torque, resistances and power losses

The torque of the machine consists of the fundamental torque  $T_1$  and the reluctance torque  $T_{rel}$ :  $T = T_1 + T_{rel}$ . According to [7] they can be calculated by equations

$$T_1 = \frac{m}{2\pi n} \frac{U_{ph} E_{PM}}{\omega L_d} \sin \delta_a \quad (65)$$

$$T_{rel} = \frac{m}{\Omega} \frac{U_{ph}^2}{2} \left( \frac{1}{\omega L_q} - \frac{1}{\omega L_d} \right) \sin 2\delta_a \quad (66)$$

From Equation (66) it can be seen that when the machine is non-salient, i.e.  $L_d = L_q$ , the reluctance torque  $T_{rel} = 0$  and the torque becomes  $T = T_1$ . This is the case with surface magnet machines.

The resistance can be calculated using equations presented in [8]. The DC resistance is

$$R_{DC} = \frac{l_c}{\sigma_c a S_c}, \quad (67)$$

where  $l_c$  is the length of a conductor in a coil,  $\sigma_c$  is the conductivity of the conductor material and  $S_c$  is the cross sectional area of the conductor. The AC resistance is

$$R_{AC,ph} = k_R \frac{N_{ph} l_{av}}{\sigma_c S_c} \quad (68)$$

where  $k_R$  is a resistance factor that takes into account skin effect in the conductors.  $l_{av}$  is the average length of a coil turn. For low voltage machines with enamelled wires it is approximately

$$l_{av} \approx 2l + 2.4W + 0.1 \text{ m} \quad (69)$$

where  $W$  is the average coil span. For large machines with prefabricated wires the average turn length is

$$l_{av} \approx 2l + 2.8W + 0.4 \text{ m} \quad (70)$$

or

$$l_{av} \approx 2l + 2.9W + 0.3 \text{ m} \quad (71)$$

when  $U = 6 \dots 11 \text{ kV}$ . The length of a conductor in a coil  $l_c$  can be approximated  $l_c = N_c l_{av}$ . The resistance factor  $k_R$  depends on the reduced conductor height that satisfies

$$\xi = h_{c0} \sqrt{\frac{1}{2} \omega \mu_0 \sigma_c \frac{b_{c0}}{b}} \quad (72)$$

where  $h_{c0}$  and  $b_{c0}$  are the height and width of a sub-conductor, respectively. If the reduced conductor height is  $0 \leq \xi \leq 1$ , a good approximation for the resistance factor of rectangular wires is

$$k_R = 1 + \frac{z_t^2 - 0.2}{9} \xi^4. \quad (73)$$

The electrical power is

$$P_{el} = m \left( \frac{U_{ph} E_{PM}}{\omega L_d} \sin \delta_a + U_{ph}^2 \frac{L_d - L_q}{2\omega L_d L_q} \sin 2\delta_a \right). \quad (74)$$

When the electrical power is known, the load angle can be solved from Equation (74). The problem here is that the efficiency cannot be known beforehand, which means that the electrical power is in fact not known. It is possible to use the chosen initial guess of the efficiency to estimate the electrical power, but this is not a very accurate method.

Therefore another method was chosen. The electrical power of a motor is

$$P_{el} = P_{mec} + P_{loss}. \quad (75)$$

This means that if the losses can be calculated or approximated, the electrical power can be evaluated using the desired shaft power. By looking at Equations (81)-(85), it can be seen that all other losses except copper losses can be calculated at this point. In order to find the copper losses the stator current has to be known. The stator current can be calculated from its d- and q-axis components, which depend on the inductances, resistance, phase voltage, back-EMF, frequency and load angle, as can be seen from Equation (76) and (77). All of these parameters are known except the load angle, which means that the current can be considered as a function of the load angle.

Now there are two possible ways to obtain the electrical power: Equation (75) and Equation (74). Combining these two equations results in an equation from which the load angle  $\delta_a$ , can be solved.

A method to calculate the currents  $I_{d,ph}$  and  $I_{q,ph}$  is presented by Jussila [9] for non-salient pole machines.

$$I_{d,ph} = \frac{U_{ph}(\omega_s L_q \cos \delta_a - R_{ph} \sin \delta_a) - E_{PM} \omega_s L_q}{\omega_s^2 L_q L_d + R_{ph}^2} \quad (76)$$

$$I_{q,ph} = \frac{U_{ph}(R_{ph} \cos \delta_a + \omega_s L_d \sin \delta_a) - E_{PM} R_{ph}}{\omega_s^2 L_q L_d + R_{ph}^2} \quad (77)$$

The stator current is

$$I_s = \sqrt{I_{d,ph}^2 + I_{q,ph}^2}. \quad (78)$$

The maximal current density is

$$J = \frac{\frac{I_n}{a}}{S_c k_{\text{cond}}} \quad (79)$$

and the linear current density is

$$A = \frac{m N_{\text{ph}} I_s}{\pi r}, \quad (80)$$

where  $r$  is the stator inner radius. The losses consist of resistive losses in stator conductors, iron losses in the magnetic circuit, mechanical losses in the bearings, and additional losses. The resistive losses are

$$P_{\text{Cu}} = m R_{\text{ph}} I_s^2. \quad (81)$$

The iron losses are

$$P_{\text{Fe}} = m_{\text{Fe,y}} k_{\text{Fe,y}} p_{10} \hat{B}_y^2 \left(\frac{f}{50}\right)^{\frac{3}{2}} + m_{\text{Fe,t}} k_{\text{Fe,t}} p_{10} \hat{B}_t^2 \left(\frac{f}{50}\right)^{\frac{3}{2}}, \quad (82)$$

where  $m_{\text{Fe,y}}$  and  $m_{\text{Fe,t}}$  are the mass of the yoke and the teeth,  $k_{\text{Fe,y}}$  and  $k_{\text{Fe,t}}$  are empirical correction coefficients and  $p_{10}$  is a coefficient depending of the material. The mechanical losses consist of the windage and ventilation losses  $P_\rho$  and the bearing losses  $P_{\text{Br}}$ .

$$P_\rho = k_{\text{rb}} D_r (L + 0.6 \tau_p) \left(2\pi n \frac{D_r}{2}\right)^2 \quad (83)$$

$$P_{\text{Br}} = 0.5 \Omega \mu F D_{\text{Br}}, \quad (84)$$

where  $\Omega$  is the angular velocity of the shaft supported by bearing,  $\mu$  is the friction coefficient (typically 0.001-0.005),  $F$  the bearing load and  $D_{\text{Br}}$  the inner diameter of the bearing.[8]

The additional losses are very difficult to calculate or measure. One assumption is

$$P_{\text{Str}} = 0.0075 P, \quad (85)$$

where  $P$  is the nominal output power. For a motor, the output power  $P$  is the shaft power  $P_s$ . When the losses are known, the efficiency can be calculated

$$\eta = \frac{P}{P + P_h} = \frac{P}{P + P_{\text{Fe}} + P_{\text{Cu}} + P_{\text{Str}} + P_{\text{Br}} + P_\rho}. \quad (86)$$

### 2.1.9 Heat transfer

Finally, the heat transfer has to be modelled in order to make sure that the machine is not overheated. Figure 5 shows the heat flow in a surface mounted PMSM. The modelling is done by using a thermal network presented in Figure 6.

There are three different methods of heat transfer: conduction, radiation and convection. Conduction is heat transfer either by molecular interaction or between free electrons. It is possible between solids, liquids and gases.

The thermal network consists of thermal resistances  $R_{th}$ . Analogous to electrical resistances, they are defined as the ratio of the potential difference to the current, i.e. ratio of temperature difference  $\theta$  to the heat flow rate  $\Phi_{th}$ . The thermal resistance for conduction can be calculated

$$R_{th} = \frac{\theta}{\Phi_{th}} = \frac{l}{\lambda S}, \quad (87)$$

where  $l$  is the length of the conductor,  $S$  is the conducting area and  $\lambda$  is the thermal conductivity of the conductor.

The second form of heat transfer is radiation. It means electromagnetic radiation which has its wave length between 0.1 and 100  $\mu\text{m}$ . Unlike the other two heat transfer methods, radiation does not need a medium for heat exchange. The thermal resistance of radiation is analogous to that of conduction

$$R_{th} = \frac{T_1 - T_2}{\Phi_{th}} = \frac{T_1 - T_2}{\varepsilon_{thr} \sigma_{SB} (T_1^4 - T_2^4) S}, \quad (88)$$

where  $\varepsilon_{thr}$  is the relative emissivity between the emitting and absorbing surfaces,  $\sigma_{SB}$  the Stefan-Boltzmann constant,  $T_1$  the thermodynamic temperature of the radiating surface and  $T_2$  the thermodynamic temperature of the absorbing surface.

The third type of heat transfer is convection. It means heat transfer between a region of higher temperature and a region of cooler temperature via a moving fluid. Heat is always transferred simultaneously by conduction and convection. The thermal resistance of convection satisfies

$$R_{th} = \frac{\theta}{\Phi_{th}} = \frac{1}{\alpha_{th} S}, \quad (89)$$

where  $\alpha_{th}$  is the heat transfer coefficient that depends on the viscosity of the coolant, the thermal conductivity, specific heat capacity and the flow of the medium. Traditionally it has been defined by empirical relations. According to [8] the heat transfer coefficient for natural convection in the air around a horizontally mounted,

unfinned cylindrical motor of diameter  $D$  with ambient temperature close to room temperature can be calculated

$$\alpha_{\text{th}} \approx 1.32 \left(\frac{\theta}{D}\right)^{0.25} \left[\frac{\text{W}}{\text{m}^2\text{K}}\right], \quad (90)$$

where  $\theta$  [K] is the temperature difference. If the convection is forced, the convection depends of the air velocity  $v$  [m/s] and the length  $l$  [m] of the machine frame:

$$\alpha_{\text{th}} \approx 3.89 \sqrt{\frac{v}{l}} \left[\frac{\text{W}}{\text{m}^2\text{K}}\right]. \quad (91)$$

However, for a typical radial flux electrical machine, there are three significant convection coefficients. The first one is related to the frame, and the other two to the air-gap and coil ends. The latter two and particularly the coil end convection coefficient are quite complex to model. To calculate the heat transfer coefficient from the rotor to the air-gap or from the stator to the air-gap the Nusselt number  $Nu$  is needed. According to [8] it is

$$\begin{aligned} Nu &= 2 \text{ for } Ta_m < 1700 \\ Nu &= 0.128Ta_m^{0.367} \text{ for } 1700 < Ta_m < 10^4 \\ Nu &= 0.409Ta_m^{0.241} \text{ for } 10^4 < Ta_m < 10^7 \end{aligned} \quad (92)$$

$Ta_m$  is modified Taylor number  $Ta_m = \frac{Ta}{F_g}$ , when  $Ta$  is the Taylor number.

$$Ta = \frac{\rho^2 \Omega^2 r_m \delta^3}{\mu_v^2} \quad (93)$$

where  $\rho$  is the mass density of the fluid,  $\Omega$  the angular velocity of the rotor,  $r_m$  the average of the stator and rotor radii,  $\delta$  the air gap, and  $\mu_v$  the dynamic viscosity of the fluid. According to [8]  $F_g$  is close to one which means  $Ta_m \approx Ta$ . Now the heat transfer coefficient can be calculated

$$\alpha_{\text{th}} = \frac{Nu\lambda}{\delta} \quad (94)$$

The heat transfer coefficient in the coil ends is more difficult to approximate. In the space between the rotor and the end winding the heat transfer coefficient is determined by the rotation speed of the rotor. The geometry corresponds to the air-gap geometry which means that the heat transfer coefficient can be calculated using Equations (92)-(94). In the space between the end winding and the frame the speed of the air stream is much smaller than in the space between the rotor and the end winding. The flow may be assumed to be laminar which means that the convection is natural and also radiation has to be taken into account.

The thermal network consists of thermal resistances that are analogous to electrical resistances. Resistive losses, iron losses, windage losses and friction losses are represented by individual heat flow sources. The heat capacity is analogous to electric capacitance. Figure 5 represents the different types of heat transfer in a permanent magnet synchronous machine. Convection is presented with green arrows, radiation with purple arrows and conduction with red arrows. The radiation inside the machine is not taken into account in the figure.

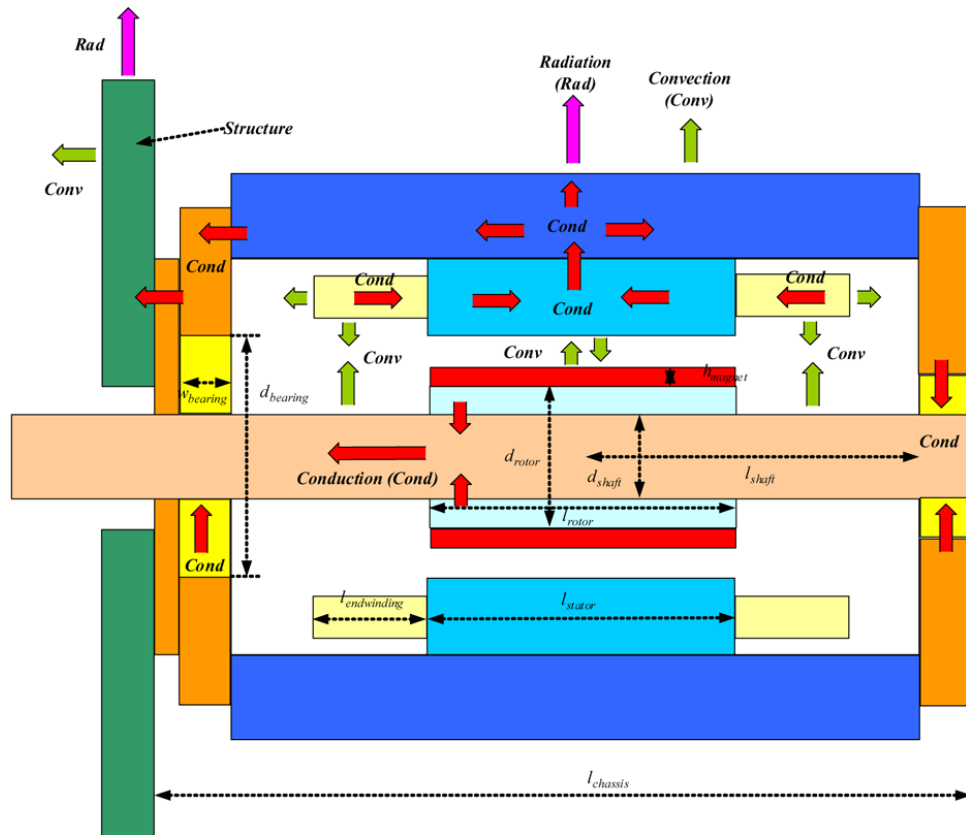


Figure 5. The heat transfer in a rotor surface mounted permanent magnet synchronous machine. [10]

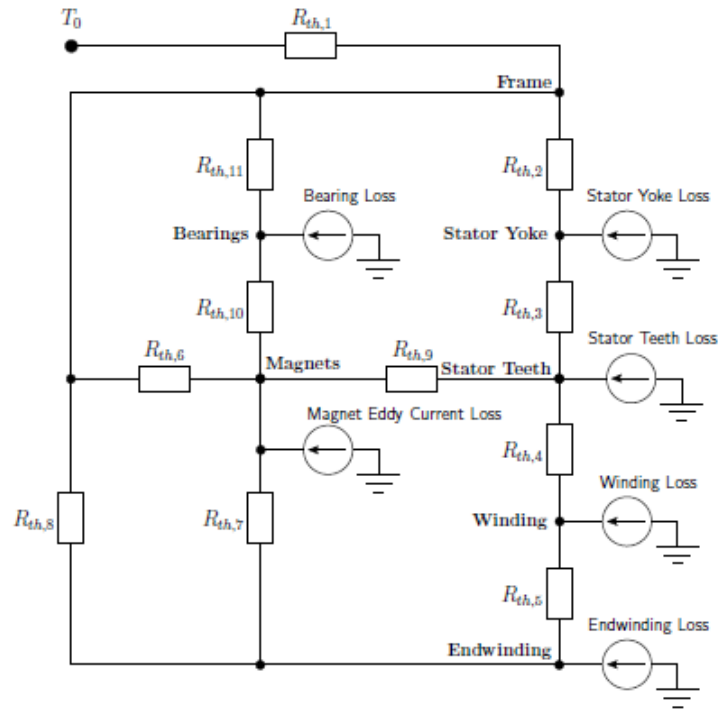


Figure 6. Thermal circuit of a surface mounted PMSM. [11]

### 2.1.10 Thermal analysis of the PMSM

The chosen thermal network for a surface mounted PMSM is presented in Figure 6. It consists of eleven thermal resistances and six heat flow sources. It has seven nodes: frame, yoke, teeth, winding, endwinding, magnets and bearings. Especially the temperature rise of the magnets is important to know, because the permanent magnets can easily demagnetize in high temperatures. The used network was originally developed by J. Lindström [12]. Originally it was intended for a water-cooled surface mounted machine, and the temperature outside the frame is assumed to be constant. Hafner et. al. [11] have presented a modification for passive cooled machines where the heat transfer between the ambient air and the frame has been modelled. Also an adaptation for an interior magnet construction has been presented [13]. In this case, the original assumption of the constant ambient temperature was considered to be accurate enough for a worst case approximation.

This network was chosen because it is relatively simple. Since the network is only used to make sure that the magnets do not overheat, a simple network is considered to be a good worst case approximation. The temperatures in the nodes of the network can be solved by writing equations for the heat flows. The equations are written in matrix form

$$\mathbf{G}_{th} \boldsymbol{\Theta} = \mathbf{P}, \quad (95)$$

where  $\mathbf{G}_{th}$  is the thermal conductance matrix of the network,  $\Theta$  is the temperature vector and  $\mathbf{P}$  is the heat flow source vector. The temperatures can be solved from Equation (95)

$$\Theta = \mathbf{G}_{th}^{-1} \mathbf{P}, \quad (96)$$

$$\mathbf{G}_{th} = \begin{bmatrix} G_{11} & -G_{th2} & 0 & 0 & -G_{th8} & -G_{th6} & -G_{th11} \\ -G_{th2} & G_{22} & -G_{th3} & 0 & 0 & 0 & 0 \\ 0 & -G_{th3} & G_{33} & -G_{th4} & 0 & -G_{th9} & 0 \\ 0 & 0 & -G_{th4} & G_{44} & -G_{th5} & 0 & 0 \\ -G_{th8} & 0 & 0 & -G_{th5} & G_{55} & -G_{th7} & 0 \\ -G_{th6} & 0 & -G_{th9} & 0 & -G_{th7} & G_{66} & -G_{th10} \\ -G_{th11} & 0 & 0 & 0 & 0 & -G_{th10} & G_{77} \end{bmatrix} \quad (97)$$

in which

$$G_{11} = G_{th1} + G_{th2} + G_{th11} + G_{th6} + G_{th8} \quad (98)$$

$$G_{22} = G_{th2} + G_{th3} \quad (99)$$

$$G_{33} = G_{th3} + G_{th4} + G_{th9} \quad (100)$$

$$G_{44} = G_{th4} + G_{th5} \quad (101)$$

$$G_{55} = G_{th5} + G_{th7} + G_{th8} \quad (102)$$

$$G_{66} = G_{th7} + G_{th6} + G_{th10} + G_{th9} \quad (103)$$

$$G_{77} = G_{th10} + G_{th11} \quad (104)$$

and  $G_{thi}$  are the individual thermal conductances of the network  $G_{thi} = \frac{1}{R_{thi}}$ .

The thermal resistance of the network consist of the thermal resistances of the different machine parts.

$$R_{th1} = \frac{1}{2} R_{thfr} \quad (105)$$

$$R_{th2} = \frac{1}{2} (R_{thfr} + R_{thy} + R_{thcy}) \quad (106)$$

$$R_{th3} = \frac{1}{2} (R_{thy} + R_{thz}) \quad (107)$$

$$R_{th4} = \frac{R_x R_y}{Ql f_r (R_x + R_y)} \left( 1 - \frac{R_{x0} R_{y0}}{720 * (R_{x0} + R_{y0})} \right) \quad (108)$$

$$R_{th5} = \frac{R_{thw}}{2Q} \quad (109)$$

$$R_{th6} = R_1 + R_2 + \frac{R_1 R_2}{R_3} \quad (110)$$

$$R_{th7} = R_2 + R_3 + \frac{R_2 R_3}{R_1} \quad (111)$$

$$R_{th8} = R_1 + R_3 + \frac{R_1 R_3}{R_2} \quad (112)$$

$$R_{th9} = R_{th\delta} + \frac{1}{2}R_{thz} + R_{thsl} + \frac{1}{2}R_{thPM} \quad (113)$$

$$R_{th10} = \frac{1}{2}R_{thPM} + R_{thins} + R_{thyr} + R_{ther} + \frac{1}{2}R_{thsh} + \frac{1}{4}R_{thb} \quad (114)$$

$$R_{th11} = \frac{1}{4}R_{thb} \quad (115)$$

Next the methods to calculate the thermal resistances of the different machine parts are explained. The stator has four thermal resistances: frame, yoke, teeth and the contact resistance between the frame and the yoke. The resistance of the frame is

$$R_{thfr} = \frac{h_{fr}}{\pi l \lambda_{Al} (D_{se} + h_{fr})}, \quad (116)$$

where  $h_{fr}$  is the height of the frame and  $\lambda_{Al}$  is thermal conductivity aluminium, which is 209 W/m·K for electro-technical aluminium [8]. The yoke thermal resistance is

$$R_{thy} = \frac{\ln \frac{D_{se}}{2} - \ln \left( \frac{D}{2} + h_z \right)}{2\pi l f_r \lambda_{Fe}} \quad (117)$$

where  $\lambda_{Fe}$  is the thermal conductivity of iron (74.7 W/m·K). The contact between the stator yoke and frame has also its own thermal resistance because of the contact of two different materials. According to [12] this contact resistance equals to equivalent gap divided by thermal conductivity and area of the gap. These parameters are rather difficult to obtain so the contact resistance is assumed to be equal to the thermal resistance of the yoke. The thermal resistance for the teeth is according to [12] an integral

$$R_{\text{thz}} = \int_0^{h_z} \frac{1}{\lambda_{\text{Fe}} Q f_r l x_z(y)} dy \quad (118)$$

where  $x_z(y)$  is the tooth length at height  $y$ . In this case the tooth length is equal everywhere except at the tooth tip. This is considered to be a minor deflection of the tooth width, and the tooth is assumed to have equal width everywhere. This means that the resistance becomes

$$R_{\text{thz}} = \frac{h_z}{\lambda_{\text{Fe}} Q f_r l b_z} \quad (119)$$

Equation (119) gives a single resistance for all the stator teeth. Next the thermal resistances from internal air to the frame  $R_1$ , rotor  $R_2$  and end winding  $R_3$  are calculated.

$$R_1 = \frac{1}{\alpha_1 A_1}, \quad (120)$$

where  $\alpha_1$  is empirically defined heat transfer coefficient

$$\alpha_1 = 15 + 6.75^{0.65} + v_r^{0.65} \text{ [W/m}^2\text{K]} \quad (121)$$

and  $A_1$  is the area exposed to convection.

$$A_1 = 2A_{\text{es}} + A_{\text{if}} \quad (122)$$

$A_{\text{es}}$  is the internal end shield area and  $A_{\text{if}}$  is the internal frame area. These can be calculated from machine dimensions.  $R_2$  is the thermal resistance between the rotor and the internal air.

$$R_2 = \frac{1}{\alpha_2 A_2} \quad (123)$$

where  $\alpha_2$  is an experimental coefficient

$$\alpha_2 = (16.5[\text{Ws/m}])^{0.65} v_r^{0.65} / \text{m}^2\text{K} \quad (124)$$

and  $A_2$  is again the area exposed to convection. According to [12], it can be calculated

$$A_2 = 2b_{\text{fin}} h_{\text{fin}} n_{\text{fin}} + \pi r_\delta^2, \quad (125)$$

where  $r_\delta$  is the air-gap radius and  $b_{\text{fin}}$ ,  $h_{\text{fin}}$  and  $n_{\text{fin}}$  are the width, height and number of the cooling fins of the rotor. If the rotor is unfinned, it means that  $A_2 = \pi r_\delta^2$ .

Resistance  $R_3$  is the thermal resistance between the end winding and the internal air.

$$R_3 = \frac{1}{\alpha_3 A_3} \quad (126)$$

$A_3$  is the area of the end winding and  $\alpha_3$  is an empirical heat transfer coefficient.

$$\alpha_3 = 6.5 \text{W/m}^2\text{K} + (5.25[\text{s/m}])^{0.65} v_r^{0.6} / \text{m}^2\text{K} \quad (127)$$

Because the temperature of the internal air of the motor is not required as a result, the thermal network can be simplified by making a wye-delta transform for resistances  $R_1, R_2$  and  $R_3$ . Thermal resistances  $R_{\text{th}6}, R_{\text{th}7}$  and  $R_{\text{th}8}$  are transformed from  $R_1, R_2$  and  $R_3$ .

$R_\delta$  is the thermal resistance of the air-gap. It can be calculated using equation

$$R_\delta = \frac{1}{\alpha_\delta 2\pi r_\delta l' f_r'} \quad (128)$$

where  $\alpha_\delta$  is the heat transfer coefficient for the air-gap.

$$\alpha_\delta = \frac{Nu \lambda_A}{2\delta} \quad (129)$$

$Nu$  is the Nusselt number

$$Nu = 0.409(Ta)_m^{0.241} - 137(Ta)_m^{-0.75} \quad (130)$$

and  $(Ta)_m$  is the modified Taylor number. [12]

$$(Ta)_m = \frac{\Omega^2 r_\delta \delta^3}{v_A^2} \quad (131)$$

in which  $v_A$  is the kinematic viscosity of air. It is temperature dependent which means that the temperature in the air-gap has to be estimated. If the modified Taylor number becomes smaller than 1740, the airflow is considered to be without Taylor vortices, and the Nusselt number is then 2.

The thermal resistance of the permanent magnets is

$$R_{\text{thPM}} = \frac{\ln\left(\frac{D_r}{2} + l_m\right) - \ln\left(\frac{D_{ri}}{2}\right)}{2\pi l f_r \lambda_{\text{PM}}} \frac{2\pi}{2pl_p} \quad (132)$$

where  $\lambda_{\text{PM}}$  is the thermal conductivity of the permanent magnet material.  $R_{\text{thins}}$  is the thermal resistance of the insulation between the magnets and the rotor yoke.

$$R_{\text{thins}} = \frac{d_{\text{Ir}}}{\pi D_{\text{r}} l_{\text{f}} \lambda_{\text{Ir}}} \frac{2\pi}{2pl_{\text{p}}}, \quad (133)$$

where  $d_{\text{Ir}}$  is the thickness of the insulation layer and  $\lambda_{\text{Ir}}$  is the thermal conductivity of the insulation material. The thermal resistance of the rotor yoke is

$$R_{\text{thyr}} = \frac{\ln(D_{\text{r}}) - \ln\left(\frac{D_{\text{ri}}}{2}\right)}{2\pi f_{\text{r}} l \lambda_{\text{Fe}}} \quad (134)$$

The contact resistance between the rotor core and the shaft  $R_{\text{thcr}}$  is assumed to be equal to that of the rotor core.

It is assumed that the heat flow in the shaft goes to the axial direction. The thermal resistance of the shaft is

$$R_{\text{thsh}} = \frac{l_{\text{bb}}}{\pi \left(\frac{D_{\text{ri}}}{2}\right)^2 \lambda_{\text{sh}}}, \quad (135)$$

where  $\lambda_{\text{sh}}$  is the thermal conductivity of the shaft and  $l_{\text{bb}}$  is the distance between the two bearings.  $R_{\text{thb}}$  is the thermal resistance of one bearing

$$R_{\text{thb}} = k_1(0.12 - k_2 d_{\text{b}})(33 - k_3 \Omega d_{\text{b}}), \quad (136)$$

where  $k_n$  are empirical coefficients. According to [14] they are valid only if  $46 \text{ mm} \leq d_{\text{b}} \leq 76 \text{ mm}$  and  $\omega d_{\text{b}} \leq 14.5 \frac{\text{m}}{\text{s}}$ .

**Table 1. Explanation for the different thermal resistances.**

<b>Symbol</b>	<b>Thermal resistance</b>
$R_{thfr}$	Frame
$R_{thy}$	Stator yoke
$R_{thcy}$	Contact resistance between the yoke and the frame
$R_{thz}$	Teeth
$R_x, R_y$	Per unit length resistances for Equation (108).
$R_{x0}, R_{y0}$	Slot material resistances (equivalent rectangular slot)
$R_{thw}$	Winding
$R_1$	Between frame and internal air
$R_2$	Between rotor and internal air
$R_3$	Between end winding and internal air
$R_{th\delta}$	Air-gap
$R_{thsl}$	Retaining sleeve
$R_{thPM}$	Permanent magnets
$R_{thins}$	Insulation between magnets and rotor yoke
$R_{thyr}$	Rotor yoke
$R_{thcr}$	Contact between the rotor core and the shaft
$R_{thsh}$	Shaft, axial
$R_{thb}$	One bearing

## 2.2 MATLAB implementation

A dimensioning tool for surface mounted permanent magnet synchronous machines was implemented using the MATLAB software. The flow chart of the program is presented in Figure 7.

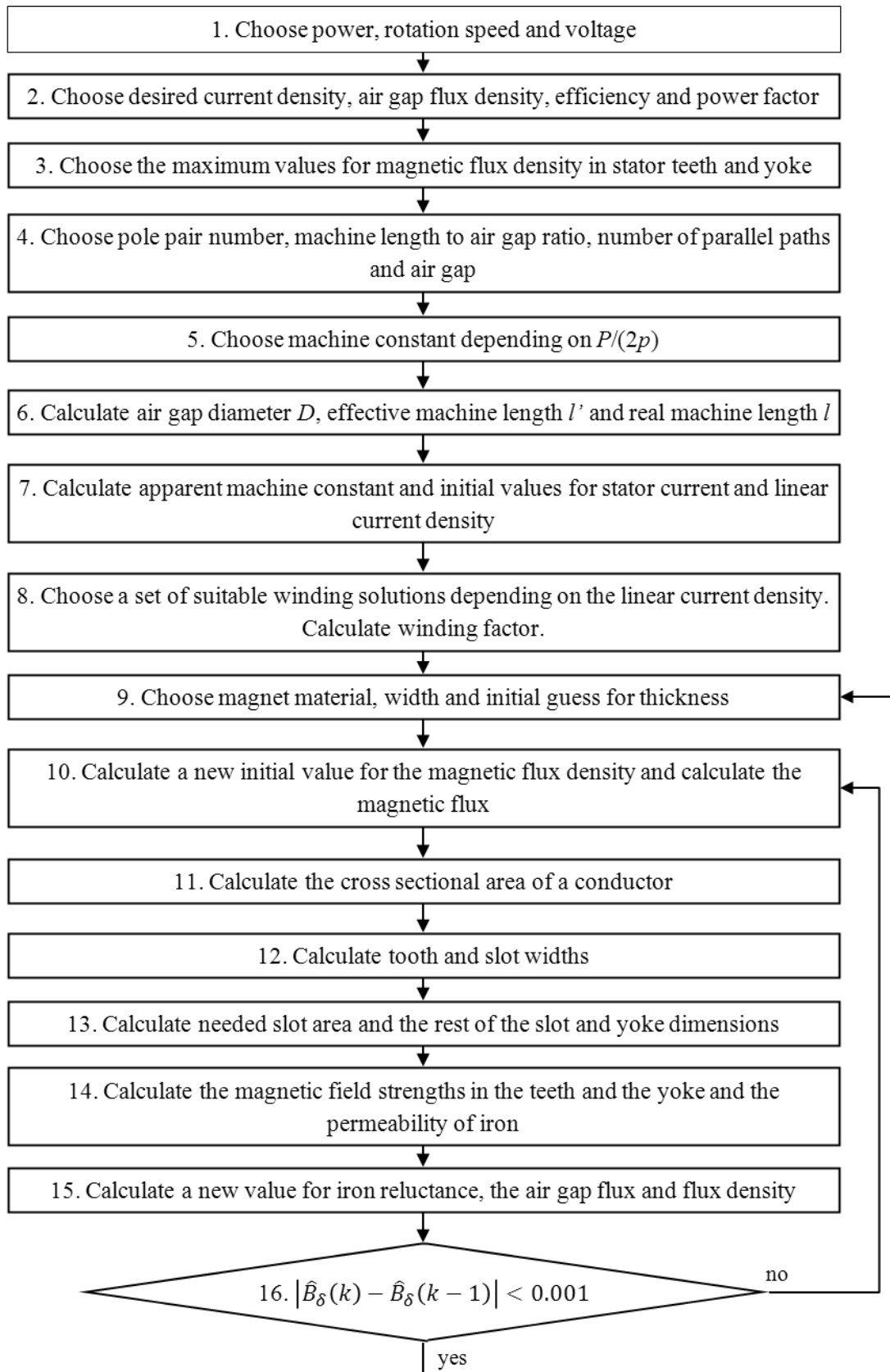
The initial parameters are chosen during steps 1-4. These parameters are quite free to choose. At step 5 the machine constant that depends on the pole power is defined. The program does it automatically according to a figure presented on page 289 in [8], but it is also possible to make the choice manually. At step 6 some of the main mechanical dimensions are defined. These are machine length, stator inner diameter and the effective machine length. The apparent machine constant and initial values for stator current and linear current density are calculated during step 7 using Equations (5) and (6).

At step 8 a suitable winding is chosen based on the estimated linear current density value. The winding is a single layer winding. The magnet material, magnet width and a guess for the magnet thickness are chosen during step 9.

At step 10 a new value for magnetic flux density is calculated using Equation (6). The dimensions of the stator slots are calculated during steps 11-13. At steps 14 and 15, new values for the air gap flux and flux density are defined by calculating

the iron reluctance. Steps 11-15 are repeated until the air gap flux does not change more than 0.001 T. At step 17 the back induced EMF is calculated using Equation (19). If the back-EMF is close to the phase voltage, the magnets are thick enough. Otherwise steps 10-17 have to be recalculated with thicker magnets. The rest of the machine properties are calculated during steps 19-23 as presented in Section 2.1.8

The thermal network is also implemented with MATLAB. It follows the equations presented in Section 2.1.10.



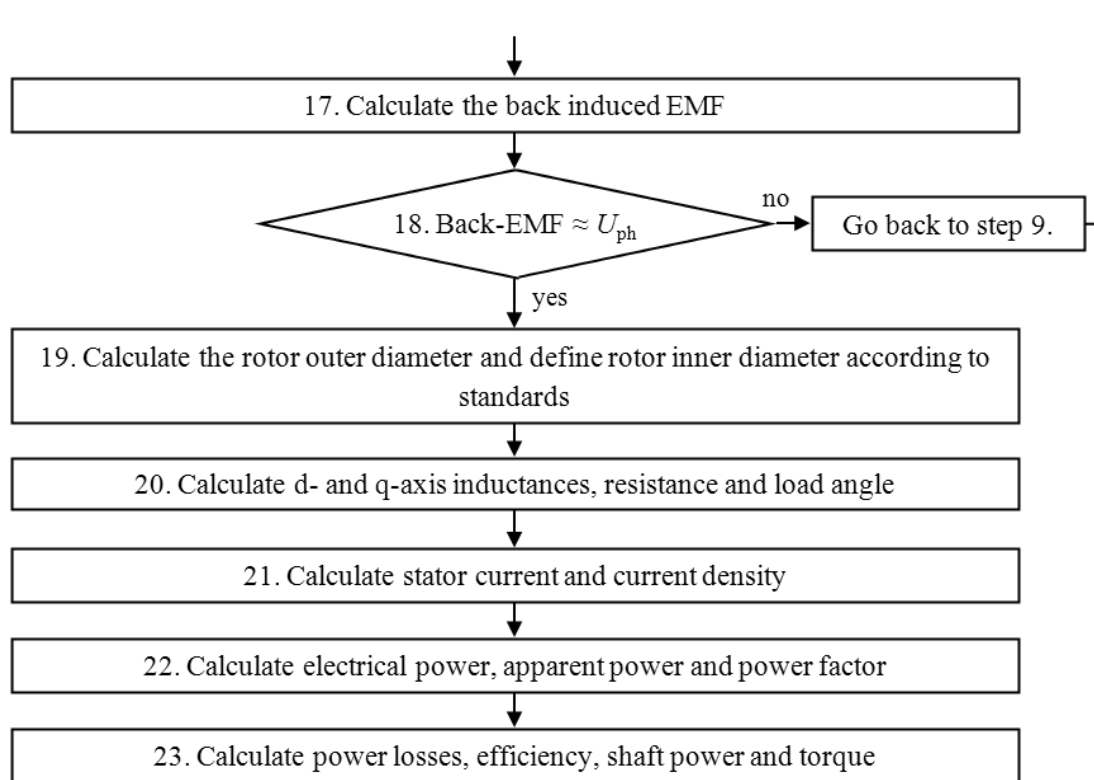


**Figure 7. The flowchart of the dimensioning tool.**

### 2.3 Operation profile

The design tool finds a solution for given input parameters. These parameters are typically those for the rated operating point. Usually electrical machines are operated at other conditions as well. This means that the machine has to have good characteristics also for example, at lower rotation speeds than the rated speed. The surface magnet machines are not usually used in rotation speeds higher than the rated one, because that would require field weakening. With permanent magnets mounted to the rotor surface, the air gap flux is constant, because it is produced by the magnets. This makes the surface mounted PMSM quite poor in field weakening.

To ensure that the design that is obtained is truly feasible, it should be tested in other operation points as well. Therefore, a method to calculate an operational profile for a design is implemented. The method enables the calculation of the load angle, stator current, electrical power, efficiency and power factor in different operation points.

If the operation point changes, it means that the rotation speed, voltage, power, torque, back-EMF and frequency change. The relation between the torque and the mechanical power is  $P = 2\pi nT$ . It is assumed that the voltage is proportional to the rotation speed. The back-induced EMF depends on the number of coil turns in a phase, magnetic flux in the air gap and frequency. In a permanent magnet machine, the air gap flux is constant because it is produced by the permanent magnets. This means that the only changing parameter is the frequency.

All other parameters can be calculated if the load angle  $\delta_a$  is known. The losses depend on the machine parameters and rotation speed. In the chosen operating point, they can be approximated because the machine parameters are known. When the load angle is defined, it is possible to solve the stator current, efficiency, power factor and electrical power in the operating point.

The interesting results from the analysis are the efficiency and power factor at different rotation loadings. If the machine is operating at lower rotation speeds than the rated speed, the efficiency might be worse than the nominal efficiency. By studying the operation profile, information about the overall feasibility of the design can be obtained.

The chosen operation profile is presented in Figure 8. The application is a 22 kW industrial pump. The shaft power in different operation points is presented as a function of rotation speed. The nominal voltage of the machine is 400 V. The percentages for the operation points are presented in Table 2. Using these it is possible to calculate a weighted average of the efficiencies and power factors. The average efficiency and power factor over the whole working period are obtained

$$\eta_{\text{ave}} = \frac{\sum_i \eta_i t_i}{t_{\text{wp}}}, \quad (137)$$

$$\cos \varphi_{\text{ave}} = \frac{\sum_i \cos \varphi_i t_i}{t_{\text{wp}}}, \quad (138)$$

where  $\eta_i$  is the efficiency of the operation point  $i$ ,  $t_i$  is the time the machine is working at operation point  $i$  during the working period, and  $t_{\text{wp}}$  is the time of the working period.

It can be seen from Table 2 that the machine is actually operating most of its working period at lower operation speed and power than the rated values. This means that it could be possible to choose the rated shaft power smaller, for example 18 kW. However, if the working period is long, the machine might be working at 22 kW shaft power for a longer time as well. In this kind of situation, it is possible that the 18 kW machine would be overloaded, and for this reason, it was chosen to use a 22 kW machine in this study.

Example results for the operating range are presented in Figure 9. The efficiency and power factor of the investigated machine are presented as a function of the rotation speed. In this case the power factor is actually better with smaller rotation speeds. The efficiency varies between 0.9563 and 0.9615 and the power factor varies between 0.9383 and 0.9994. This shows one of the advantages of permanent magnet synchronous machines: they can provide good efficiency and power factor also with smaller rotation speeds.

**Table 2. Operation profile.**

<b>Percentage of the working period [%]</b>	<b>Percentage of the nominal power [%]</b>
<b>5</b>	100
<b>20</b>	75
<b>25</b>	50
<b>10</b>	35
<b>5</b>	20
<b>5</b>	10
<b>30</b>	0

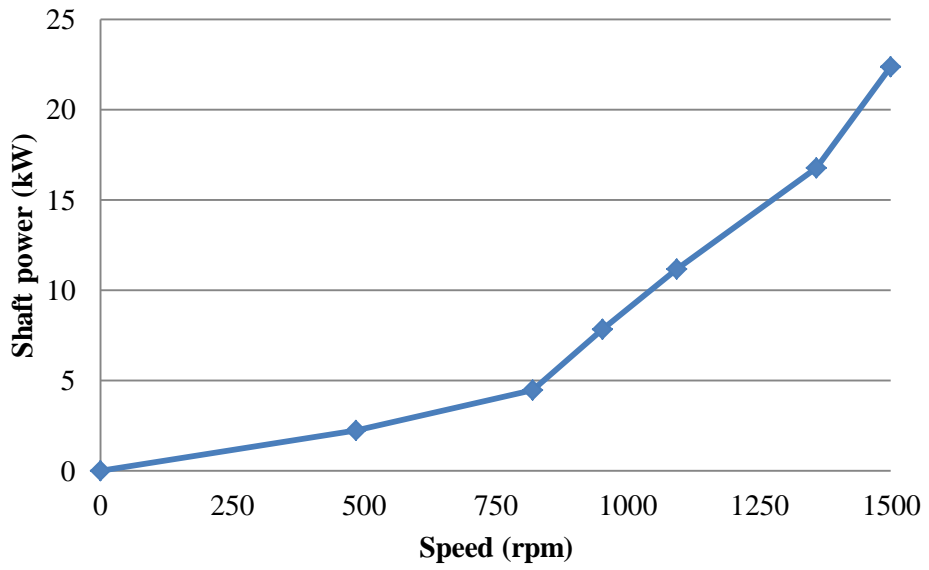


**Figure 8. The shaft power versus the rotation speed of the industrial pump that was chosen for the application.**

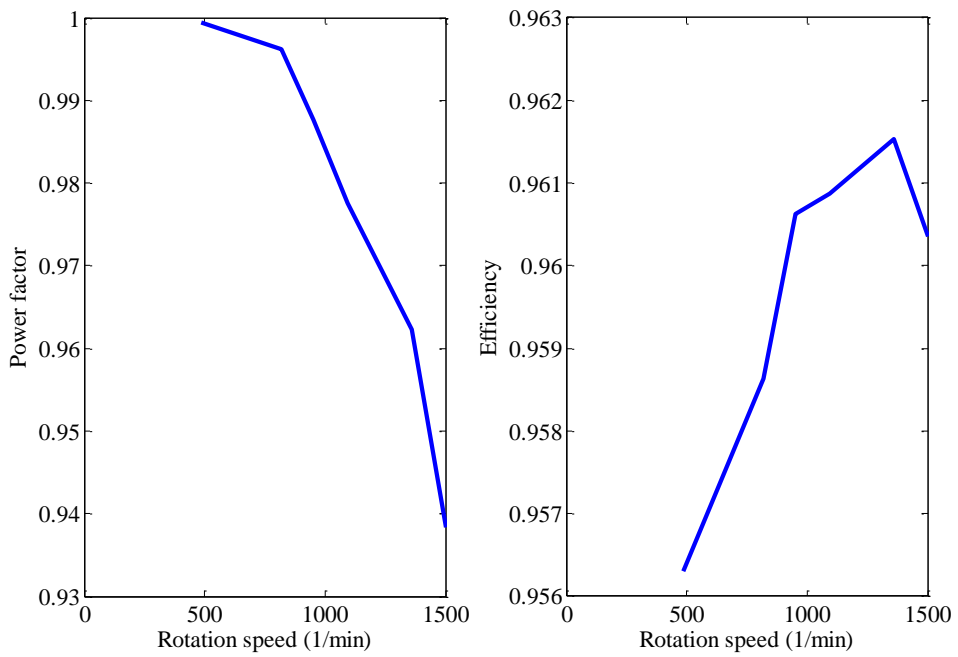


**Figure 9. Example results for the operating range.**

## 3 Results

### 3.1 Validation of the dimensioning tool

After completing the dimensioning tool, the results had to be validated for ensuring that the tool is working correctly. To be able to make conclusions, it is essential that the results calculated with the dimensioning tool can be trusted.

The validation method was to first do the dimensioning with the implemented tool and then verify the result using finite element method (FEM). The Flux2D software of CEDRAT [15] was used for the FEM modelling and calculation. This way it is possible to study more accurately how the obtained solution behaves. The results calculated with FEM are compared with the ones obtained using the dimensioning tool. This is done with three different machine constructions. The results should be at least close to those obtained by the dimensioning tool. Some small differences might appear since the dimensioning tool is based only on analytical equations which include a lot of approximations. With FEM some of the machine properties, for example magnetic flux densities and losses can be modelled more accurately. Therefore it is enough if the results are close to each other.

The FEM results were calculated by Janne Keränen [16]. Three different designs were tested: one with two poles, one with eight poles and one with 14 poles. The dimensions and other parameters for the models are presented in Appendix 2. The validation results are shown in Table 3, Table 4 and Table 5 for the 2-pole, 8-pole and 14-pole designs, respectively.

For the 2-pole machine it can be seen that the FEM results and the dimensioning tool results seem to be rather close to each other. The shaft power and torque agree well with the analytically obtained values: the difference is less than 1 % of the dimensioning tool results. Also the phase voltage and current of the FEM calculations agree well with the analytical results. The back-EMF is also somewhat close to the original value. However, it seems that the larger the pole pair number is the smaller back-EMF the FEM calculations give. It was also observed that if there are very many poles, the leakage flux from a magnet to its neighbouring magnet becomes larger. This is not taken into account by the dimensioning tool, and can therefore be one explanation to the difference in the back-EMF.

For 2- and 8-pole machines, efficiency and power factor are slightly smaller when calculated with the dimensioning tool than with Flux2D. In the case of the efficiency, some difference occurs because the Flux2D does not take into account the core losses when calculating the efficiency. Therefore Flux2D can give larger

efficiency than the dimensioning tool. For the 14-pole design, the power factor is larger when calculated with the dimensioning tool than the one obtained with FEM.

When comparing the power factors it must be taken into account that the dimensioning tool assumes that the supply voltage is sinusoidal. This means that the harmonics created by for instance a frequency converter are not taken into account. In Flux2D, this kind of assumption has not been made which may cause a difference between the power factors.

The losses seem to be slightly different when calculated with Flux2D than what the dimensioning tool gives. For the two-pole design, the difference is 14 % in the copper losses and 21 % in the iron losses. For the 8-pole design the results agree well with each other: the differences are 0.3 % for the copper losses and 2.0 % for the iron losses. For the 14-pole design, the difference between the copper losses calculated with Flux2D and with the dimensioning tool is less than 1 %. On the other hand, the iron losses obtained with Flux2D are half of the iron losses given by the dimensioning tool.

One explanation for the differences in the iron losses is that the calculation method is quite different. The dimensioning tool uses Equation (82) for calculating the iron losses. The equation gives an approximation for total iron losses, including both hysteresis and eddy current losses. The accurate calculation of the iron losses is in any case rather difficult and requires modelling the physical phenomena in the iron. Therefore also the iron losses obtained with Flux2D are also an approximation, although possibly somewhat more accurate.

**Table 3. Validation results for the 2-pole design.**

<b>Parameter</b>	<b>Flux2D</b>	<b>Dimensioning tool</b>
<b>Back-EMF voltage [V]</b>	240.1	230.9
<b>Torque [Nm]</b>	139.5	140.5
<b>Stator current [A]</b>	33.3	35.9
<b>Phase voltage [V]</b>	232.0	230.9
<b>Electric power [kW]</b>	22.6	23.2
<b>Mechanical power [kW]</b>	21.9	22.0
<b>Efficiency rate</b>	0.970	0.947
<b>Power factor</b>	0.976	0.936
<b>Ohmic losses [W]</b>	420.3	489.6
<b>Core losses [W]</b>	211.9	174.9
<b>Back-EMF air-gap flux [Wb]</b>	0.0354	-
<b>Nominal point air-gap flux [Wb]</b>	0.0273	0.0339

Table 4. Validation results for the 8-pole model.

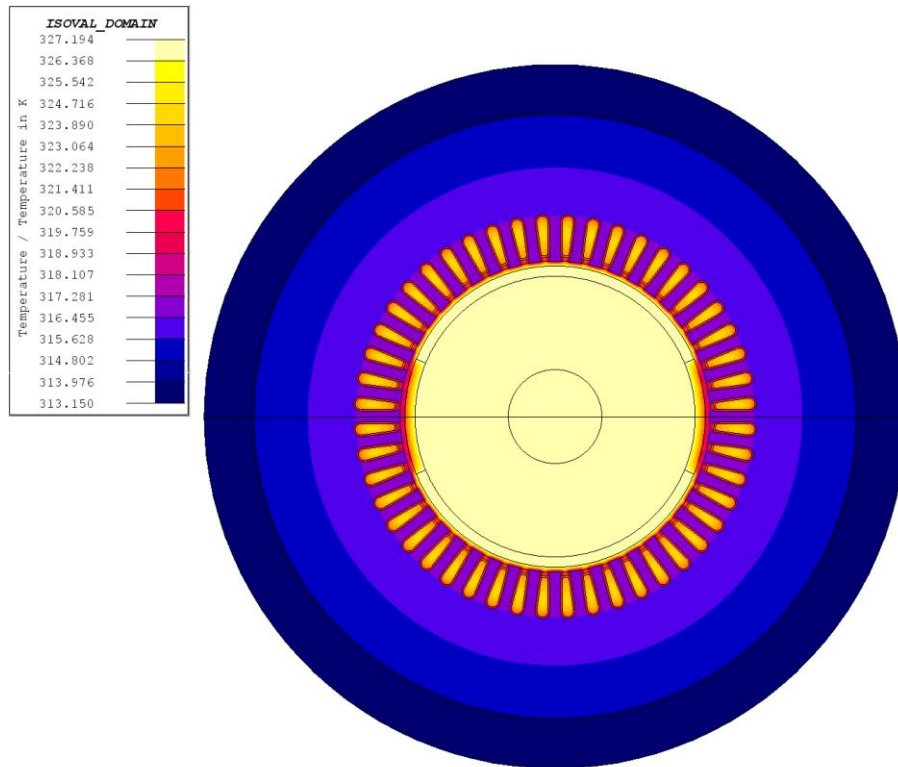
Parameter	Flux2D	Dimensioning tool
Back-EMF voltage [V]	229.2	230.9
Torque [Nm]	141.0	141.2
Stator current [A]	32.6	38.0
Phase voltage [V]	231.0	231.0
Electric power [kW]	22.5	24.1
Mechanical power [kW]	22.2	22.9
Efficiency rate	0.985	0.949
Power factor	0.996	0.889
Ohmic losses [W]	279.8	378.9
Core losses [W]	362.7	355.9
Back-EMF air-gap flux [Wb]	0.0578	-
Nominal point air-gap flux [Wb]	0.0565	0.0055

Table 5. Validation results for the 14-pole machine.

Parameter	Flux2D	Dimensioning tool
Back-EMF voltage [V]	217.1	230.9
Torque [Nm]	142.3	142.2
Stator current [A]	34.4	34.5
Phase voltage [V]	231.6	230.9
Electric power [kW]	23.1	23.9
Mechanical power [kW]	22.4	22.3
Efficiency rate	0.968	0.935
Power factor	0.968	0.999
Ohmic losses [W]	613.4	619.1
Core losses [W]	304.5	640.0
Back-EMF air-gap flux [Wb]	0.0026	-
Nominal point air-gap flux [Wb]	0.0026	0.0027

Also the thermal network is validated using the Flux2D. The thermal modelling can be done much more precisely with the software, but since the thermal network used by the dimensioning tool is quite simple, it was decided that a simple analysis would be sufficient also with Flux2D. The temperatures of the different parts of the two-pole machine can be seen in Figure 10. Because the model is 2D, the endwinding and bearings are not included in the temperature analysis. However, the effect of the

endwinding and the heat transfer along the shaft are taken into account when calculating the other temperatures.



**Figure 10.** The temperatures in the different machine parts calculated using FEM.

The results of the temperature analysis of the dimensioning tool and Flux2D are presented in Table 6. It can be seen that all other values agree well, but the temperature of the permanent magnets is slightly colder when calculated with Flux2D than what is obtained with the dimensioning tool. The possible explanation could be that the dimensioning tool gives larger eddy current losses for the permanent magnets than Flux2D. Particularly if the magnets are very thin, the dimensioning tool gives often high eddy current losses for the magnets.

**Table 6.** Comparison of the temperature analysis between the dimensioning tool and Flux2D.

<b>Machine part</b>	<b>Flux2D</b>	<b>Dimensioning tool</b>
<b>Frame (°C)</b>	40.0	40.0
<b>Yoke (°C)</b>	42.5	42.3
<b>Teeth (°C)</b>	44.1	44.6
<b>Winding (°C)</b>	51.0	51.8
<b>Endwinding (°C)</b>	-	75.7
<b>Magnets (°C)</b>	54.0	59.7
<b>Bearings (°C)</b>	-	41.9

### 3.2 Description of the calculation process of results

The tool was implemented to analyse the effect of the design parameters to the machine properties. Therefore a data set of possible design solutions for a surface mounted permanent magnet synchronous machine was calculated by varying the design parameters. It was chosen to keep the desired shaft power, rotation speed and voltage constant since these often depend of the system the machine is intended for. The varied parameters were chosen to be the pole pair number, machine length to air gap diameter ratio  $\chi$ , initial values for the current density and the air gap flux density, size of the air gap and relative magnet width. The initial values of the current density and the air gap flux density are approximations of their final values. Both of these quantities are recalculated during the design process. However, the initial values affect the final values and therefore they can also affect to other machine properties. It was assumed that the magnetic flux densities in the stator yoke and teeth are linearly depending of the flux density in the air gap. The number of parallel paths was chosen to be one. Also the iron and copper filling factors were fixed.

The objective of the design was chosen to be a 22 kW machine with nominal rotation speed of 1500 rpm and 400 V mains voltage. The values given to the initial parameters are presented in Table 7. The values for air gap flux density and current density are based on values presented in [8].

**Table 7. Initial parameters**

<b>Design parameter</b>	<b>Range of tested values</b>
<b>Pole pair number</b>	1 – 14
$\chi$	0.5 – 2.0
<b>Air gap</b>	0.5 mm – 2 mm
<b>Relative magnet width</b>	0.6 – 0.9
<b>Current density, initial value</b>	2.5 – 6.5 A/mm <sup>2</sup>
<b>Air gap flux density, initial value</b>	0.7 – 1 T

The result data contains all the main dimensions and properties of a surface permanent magnet machine. These depend of the given initial parameters. When the initial parameters are changed, different solutions are obtained. Some of the solutions are better than other ones. Because any optimization is not used, there are also a lot of unreasonable solutions. It is just not possible to produce a working PMSM design with all possible combinations of design parameters. Sometimes the design procedure fails to calculate any design with the given initial conditions and sometimes the obtained solution is just unreasonable, for example it does not produce the desired shaft power. The temperature rise might be too high. This is critical especially because the permanent magnets can easily demagnetize in high

temperatures. Therefore, checking is needed before the analysis to exclude unreasonable solutions from the analysis. The checked properties are the produced shaft power, the current density and linear current density, the temperature rise in the magnets and the stator yoke height.

Because there are many varying parameters and a lot of data, it is difficult to represent the data illustratively. A lot of different plotting methods were tested and two were considered to be the most useful. One way is to plot the different solutions as a function of certain properties, for example efficiency or mass. Another way is to plot the interesting machine properties as a function of the initial parameters. Either single solutions can be plotted or minimum, mean and maximum values of the investigated parameter can be calculated from the solution data set. It was decided to plot the investigated four parameters as functions of each other. The four properties were also represented as a function of the six initial parameters.

The dimensioning tool works actually best with pole pair numbers 1 – 6 because the machine constant is represented only for those pole pair numbers in [8]. It is possible to do the dimensioning for larger pole pair numbers as well, but this means that the curve has to be extrapolated.

Another problem with larger pole pair numbers is that the stator yoke often becomes very thin. The reason for this is that the stator yoke height is calculated from the chosen magnetic flux density value. If the yoke is very thin, it is not mechanically strong enough. Therefore, the solutions with very thin yoke were left out of the analysis.

This means that a smaller amount of good solutions were obtained with larger pole pair numbers than smaller ones. For example if we look at Figure 11 the largest pole pair number 14 is represented with dark blue dots. From the figure it can be seen that there are quite a lot less data points for 28 pole machines than for example 24 pole machines. In fact, 14 was the largest pole pair number that gave reasonable solutions with this dimensioning tool. The main reason for this is the automatic choice of the machine constant. If the dimensioning tool is used to calculate only one solution, the machine constant can be chosen manually, and larger pole pair numbers are possible as well.

The air gap flux densities for the stator yoke and teeth are also defined as initial parameters. To reduce the number of varying parameters, they were assumed to be linearly dependent of the flux density in the air gap. Therefore it has to be notified that the air gap flux density initial parameter actually affects also the other flux densities and not just the flux density in the air gap.

### 3.3 Machine properties explored

The most interesting machine properties are the efficiency, power factor, machine size and weight and the amount of permanent magnet material used. The calculated solutions of the result data set can be compared by observing these properties and investigating how the initial parameters affect. The functioning of the machine is investigated also in other operation points than the nominal point. Here the main interests are the average efficiency and power factor during the working period. These values are also included in the analysis. The chosen operation profile was explained in Section 2.3.

If the efficiency is poor, it means that the machine has high losses, which means that a lot of energy will be wasted. From the energy conservation point of view, the efficiency should thus be as good as possible. Typically the efficiency of a permanent magnet synchronous machine is high, about 0.9-0.95.

The power factor is the ratio of active and apparent power. A poor power factor means that the machine needs a lot of reactive power. It is possible to achieve unity power factor with a PMSM, even though sometimes lower power factors are also used to improve other machine properties. For example the amount of permanent magnet material can be reduced by allowing the back-EMF to be lower, for example 90 % of the phase voltage. This will also cause a lower power factor, but the manufacturing costs are reduced. [7] Here it must be mentioned that the supply voltage is assumed to be sinusoidal. With non-sinusoidal supply voltages, the power factor would be less than one.

The weight of the machine should preferably be as small as possible. The lighter the machine is, the less material is needed which makes the costs lower. Especially if the machine is intended for a moving solution, for example an electric vehicle, the weight of the machine can be a problem. In that kind of application part of the torque produced by the machine goes to move the machine itself. If the machine can be made to have less weight, less energy is needed to move the machine. Reduction of the amount of material used is also environmentally friendly.

The permanent magnet materials are usually expensive. For example compared to the price of copper, the price of NdFeB-magnet material is about 11 times higher [2], [3]. This means that the amount of magnet material used should be small. However, the magnets have to be thick enough to produce enough flux in the air gap. Sometimes also the eddy current losses of the magnets might become large if the magnets are small.

### 3.4 Effects of the initial design parameters

In this chapter, the obtained results are presented. The interesting properties are efficiency, power factor, machine size and the amount of permanent magnet material. For efficiency and power factor, both nominal and average values are presented. The interesting properties are presented as functions of the design parameters. Next, the effects of the investigated design parameters are presented.

#### 3.4.1 Pole pair number

The dependency of the mass of a machine on its pole pair number is presented in Figure 13. The leftmost figure represents the mass of the iron parts, i.e. the stator and rotor core. The mass of the winding is presented in the middle and the total mass of the machine in the rightmost figure in Figure 13. The pole pair number has a strong effect on the machine size. The minimum mass obtained for a two-pole solution was 120 kg whereas the minimum mass for a 28-pole solution was only 25 kg. Also the mean and maximum values of the weight of the iron parts decrease strongly when the number of poles increases. From Figure 11, it can be seen that the solutions that have two poles are considerably heavier than the other ones. This is because those designs have a smaller machine constant than designs with larger pole pair number. The definition of the machine constant is explained in Section 2.1.1 and Section 2.2. According to the figure that is presented in [8] the machine constant for two-pole machines is smaller than for other pole pair numbers. This choice makes the machine larger, since the machine constant affects the machine size.

On the other hand, the efficiency becomes worse with the solutions having more poles as can be seen from Figure 12. The best efficiency that was obtained was 0.966 with two poles whereas with 28 poles it was 0.916. The maximum power factor was 1 with all tested pole pair numbers. The power losses are presented in Figure 15, which shows the total power losses as well as the iron and copper losses. It can be observed that the iron losses become larger with larger pole pair numbers. This is quite a natural result since the iron losses are calculated using Equation (82) which depends of the frequency. Because the rotation speed is kept constant in this case, the designs with higher pole pair number need a higher supply frequency as well. The copper losses can be seen in the middle in Figure 15. It seems that there is a minimum for the copper losses somewhere around pole pair number 5. However, the total losses behave quite similarly with the iron losses. It can be also seen that with small number of poles, the copper losses are larger than the iron losses whereas with larger number of poles the iron losses become larger due to the increased frequency.

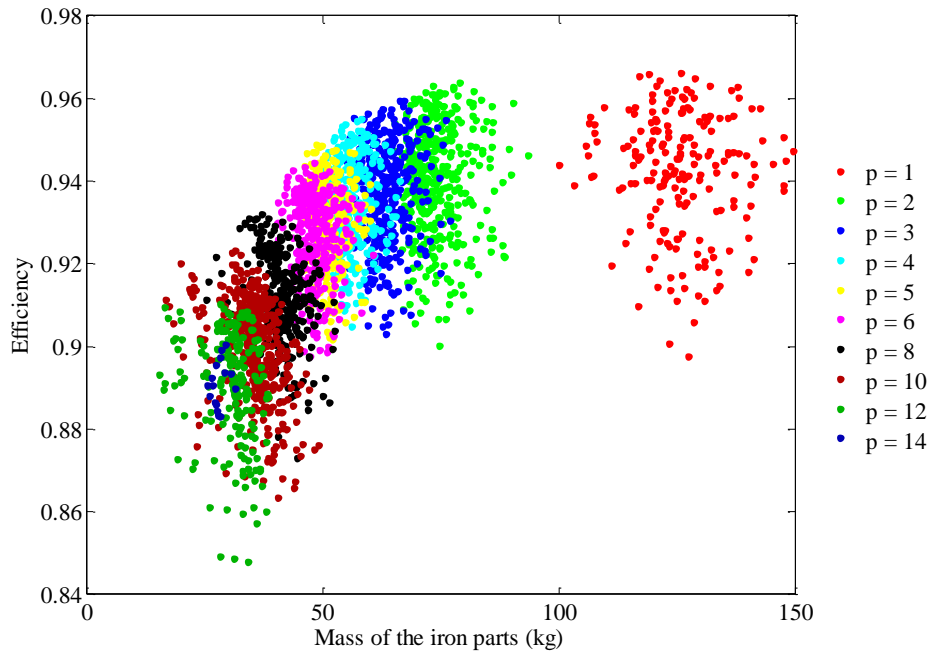


**Figure 11. Efficiency and mass of iron parts with different number of poles.**

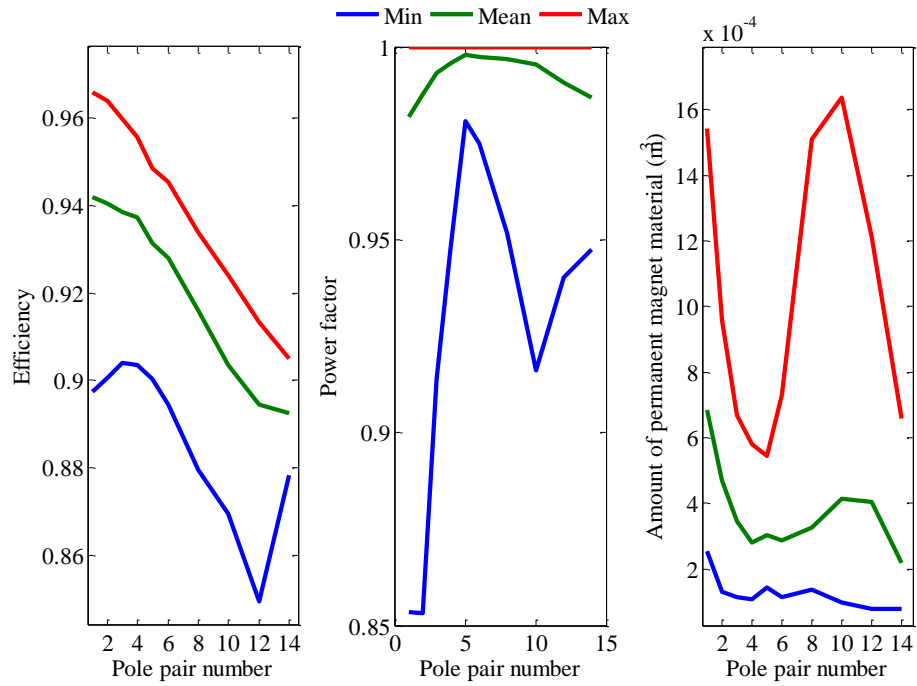


**Figure 12. The effect of the pole pair number.**

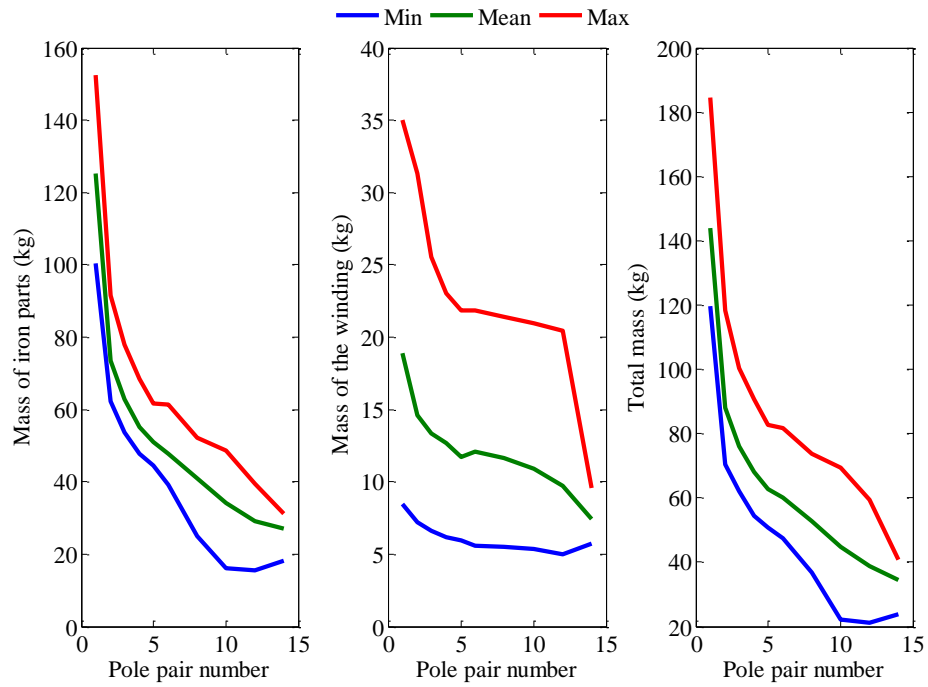


**Figure 13. The mass of the different designs as a function of the pole pair number.**

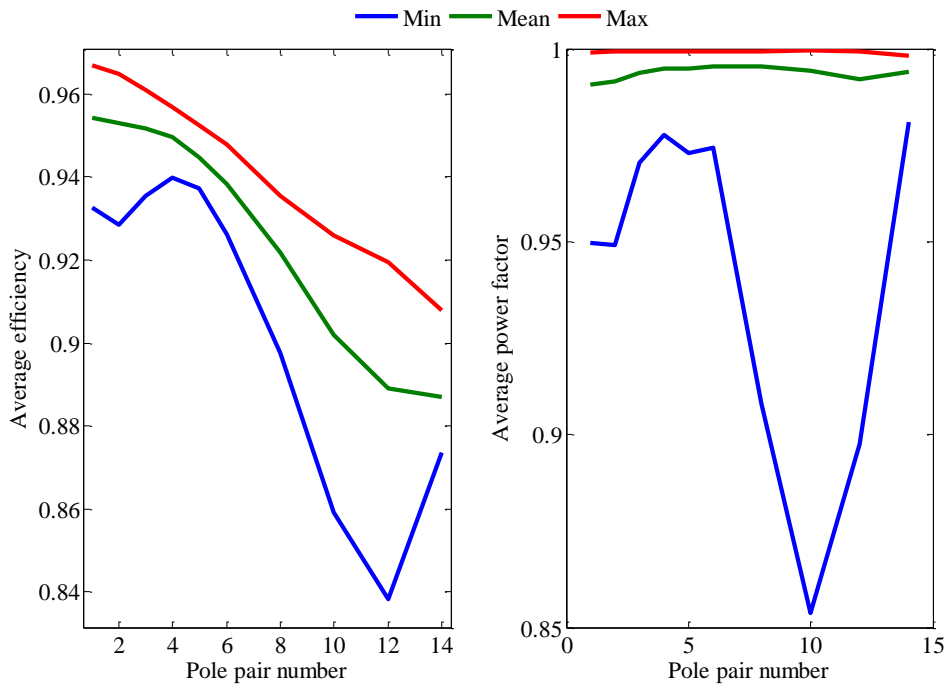


**Figure 14. Average efficiency and power factor as a function of pole pair number.**

The working temperatures of the different machine parts are represented in Figure 16. It is worth mentioning here that the temperatures of a single solution are not

presented and Figure 16 shows only the minimum, average and maximum temperatures of the set of obtained design solutions. Anyhow the temperatures seem to rise when the number of poles is increased. This is quite logical since the iron losses increase also. It can be also seen that the winding and endwinding have the highest temperature.

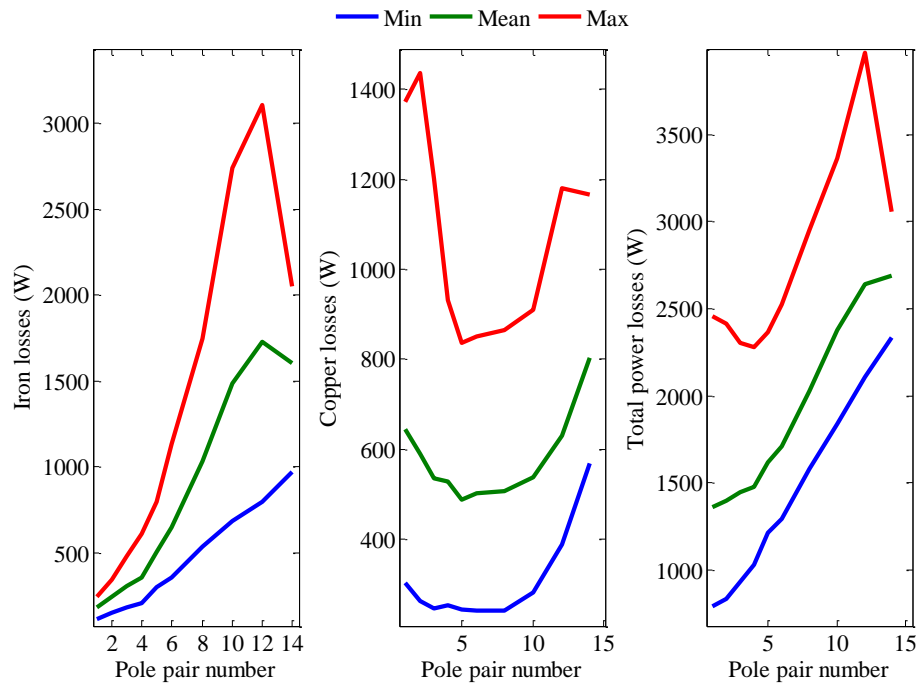


**Figure 15. Power losses as a function of the pole pair number.**

The curve for the amount of permanent magnet material used looks quite interesting (see Figure 12). It seems that less magnet material is needed with larger pole pair numbers. However, the maximum value for the volume of permanent magnets rises quite dramatically when the pole pair number is 8. It must be noticed that when studying the amount of permanent magnet material, the solutions with minimum value are optimal, and the ones with large values are expensive. Because any kind of optimization algorithm is not used, there are both good and bad solutions presented in the figures. This causes a large variation between the maximum and minimum values of some of the investigated properties. The amount of permanent magnet material depends on the magnet thickness. The dimensioning tool solves the thickness iteratively as shown in the flowchart in Figure 7 (steps 9 – 18). To be able to calculate a great amount of different solutions, the permanent magnet thickness was limited to 50 mm at maximum, which is quite a large value. This value was chosen because it ensures that the iteration does not stop too early. Sometimes it can happen that the iteration does not converge. This then means that not even magnets as thick as 50 mm are able to produce the wanted back-EMF for the design in question. This could be one possible explanation for the rapid change in the amount of permanent magnet material in Figure 12.

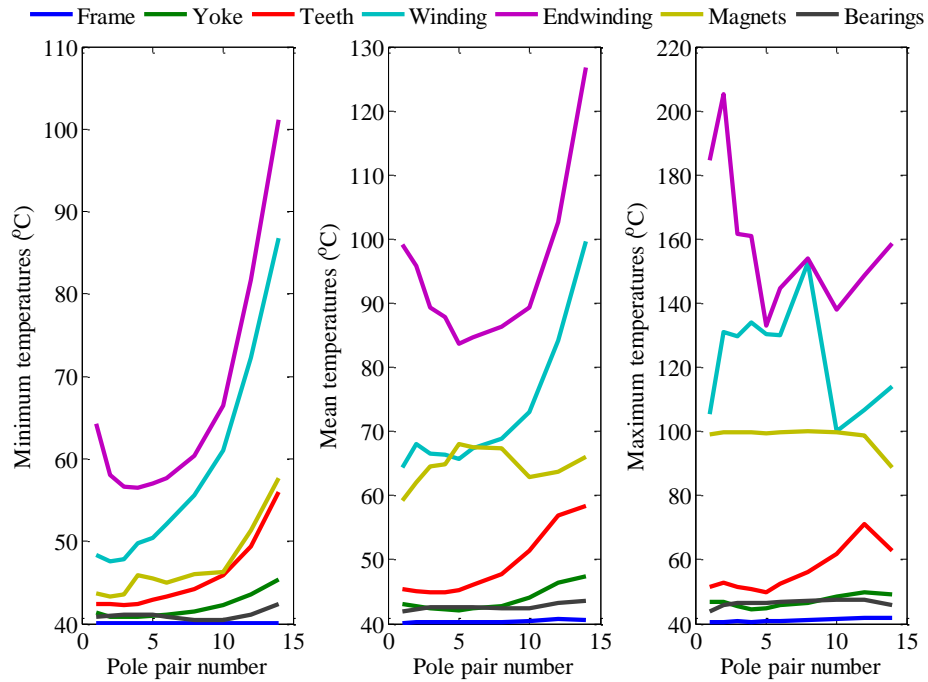


**Figure 16. The temperatures of the different machine parts as a function of the pole pair number. Minimum, mean and maximum values are presented.**

It is noteworthy too that the minimum and mean values of magnet material decrease when there are more poles. Therefore, it is possible to reduce the amount of magnet material needed by adding more poles.

### 3.4.2 Machine length to air gap diameter ratio

Figure 17 shows how the machine length to air gap ratio  $\chi$  affects the investigated machine properties. The mass of the machine is presented in Figure 18 and Figure 19 shows the average efficiency and power factor.  $\chi$  is varied from 0.5 to 2. This means that the machine length can vary between half of the air gap diameter to twice the air gap diameter. It can be seen that the machine is lighter when the air gap diameter is large compared to the machine length. For example when the machine length is only half of the air gap diameter, an average weight of 60 kg was obtained for the solutions whereas when the machine length was twice the air gap diameter the average weight was about 95 kg. Also the obtained minimum weight increased from 20 kg to 50 kg.

On the other hand, the efficiency is worse with short and thick machines than with long and thin machines although the differences are rather small. When  $\chi$  is increased from 0.5 to 2 the best obtained efficiency increases from 0.960 to 0.965. When  $\chi$  increases the amount of permanent magnet material increases as well. The maximum value of the power factor is one with every tested machine length to air

gap ratio values. The mean value is also high, above 0.98. The average efficiency (Figure 19) behaves quite similarly with the nominal efficiency.

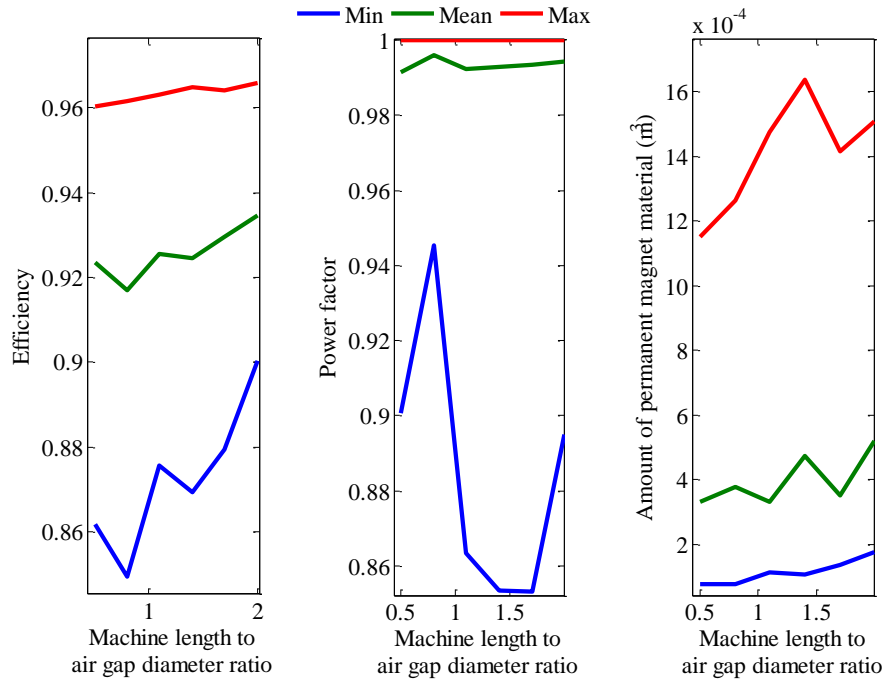


**Figure 17. The effect of the machine length to air gap diameter ratio on the nominal efficiency, power factor and permanent magnet volume.**

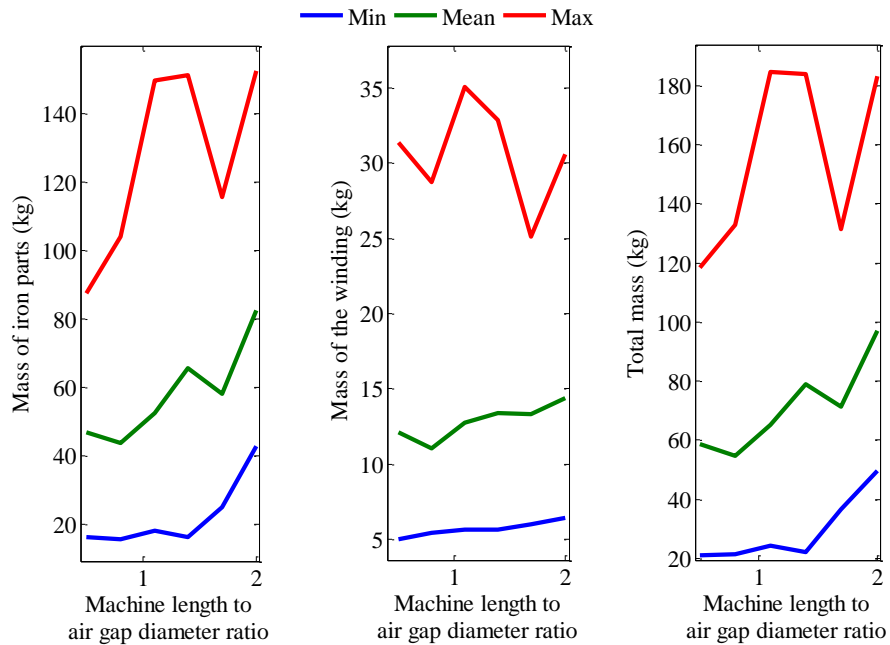


**Figure 18. The mass of the different designs as a function of the machine length to air gap diameter ratio  $\chi$ .**

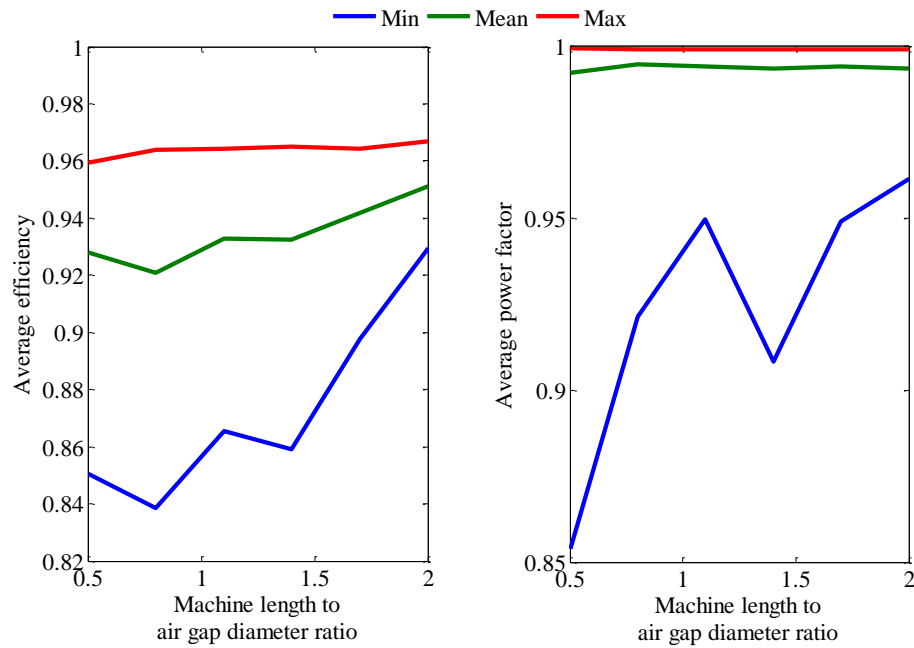


**Figure 19. The average efficiency and power factor as a function of machine length to air gap ratio.**

### 3.4.3 Air gap

The effect of the air gap length  $\delta$  on the machine properties is discussed next. The actual air gap is measured from the top surface of the permanent magnets to the bottom of the stator teeth. The lower limit for the air gap length is set by the mechanical constraints. Basically the upper limit is not as clear, but if the air gap becomes too large, the magnets cannot produce enough flux to cause the rotor to rotate.

The air gap length can be also evaluated from Equations (14) and (15) which depend on the desired shaft power of the machine. Here the air gap was considered as a free design parameter, and its value was varied. This is partly because the air gap given by (14) and (15) is very small, about 0.5 mm for a 22 kW machine with more than two poles. This is maybe some kind of theoretical minimum value for the air gap, and therefore it was used as a lowest value that was tested.

The effect of the air gap is shown in Figure 20 and Figure 21. The air gap varies from 0.5 mm to 2.5 mm. The smallest value is probably somewhat theoretical but it is close to the value obtained with Equations (14) and (15). It was still tested despite the fact that it is maybe always not realistic.

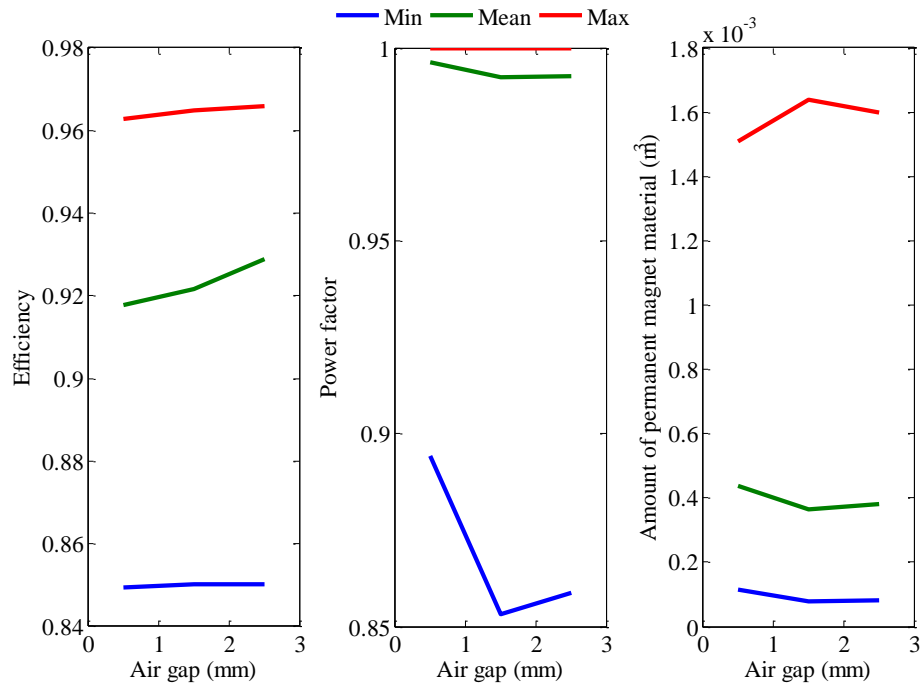


**Figure 20. The effect of the air gap to the machine properties.**

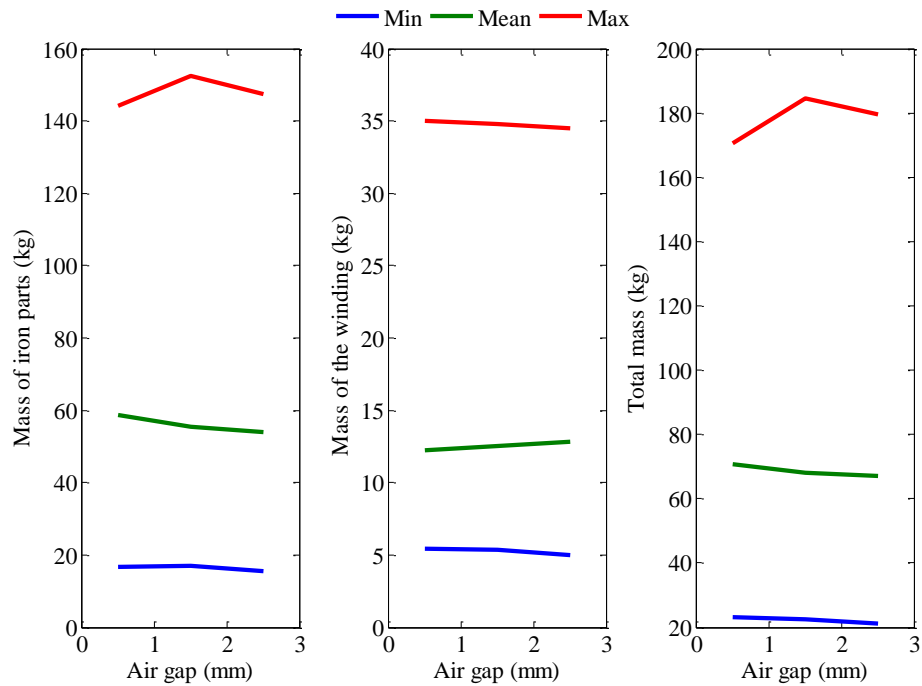


**Figure 21. The effect of the air gap on the mass of the machine.**

It can be seen from Figure 21 that the mass of the machine becomes slightly smaller with larger air gaps. However the effect is not very strong. The efficiency is better with larger air gaps although the obtained maximum value increases only slightly. The power factor is worse if the air gap is larger although the maximum value is

always one. The minimum and mean values decrease slightly when the air gap increases. The average efficiency and power factor behave similarly than the nominal values as can be seen from Figure 22.

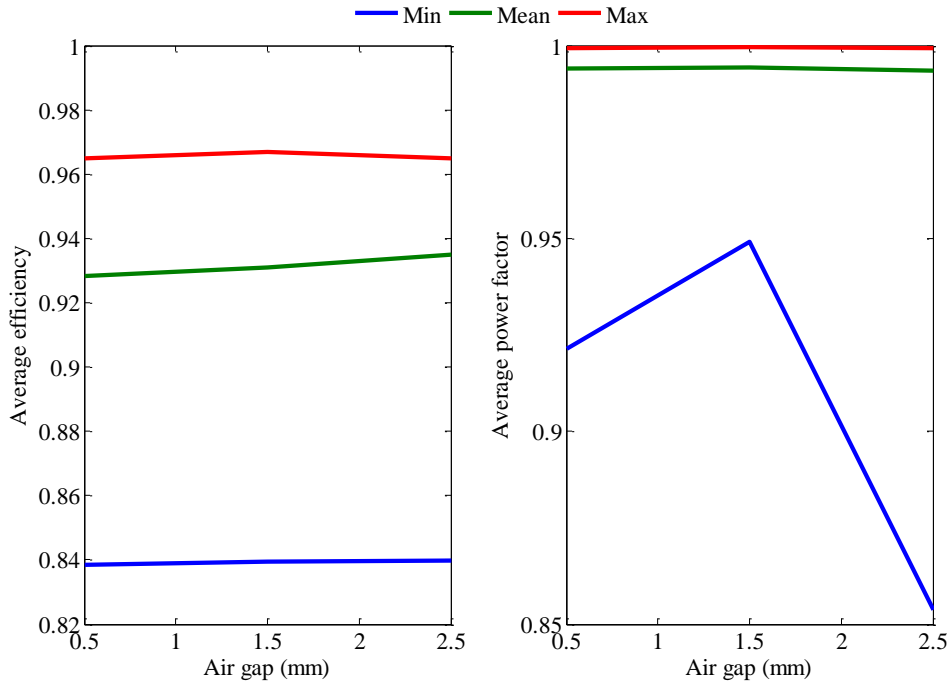


**Figure 22.** The average efficiency and power factor versus the air gap of the machine.

#### 3.4.4 Relative magnet width

The relative magnet width describes how wide the magnets are compared to the pole pitch. The actual width of the magnets is here obtained by multiplying the pole pitch by the relative magnet width. According to [9] typical relative permanent magnet width for surface mounted permanent magnet machines is about 0.8–0.85. Here the relative magnet width was varied between 0.6 and 0.9.

The effect of the relative magnet width is shown in Figure 23, Figure 24 and Figure 25. The relative magnet width does not seem to have very strong effect on any of the investigated properties. The total mass of the designs seem to increase slightly when the relative magnet width is increased. This is because of the increased mass of the iron parts. The mass of the winding is actually smaller with wider magnets. The magnet width also affects the torque ripple.

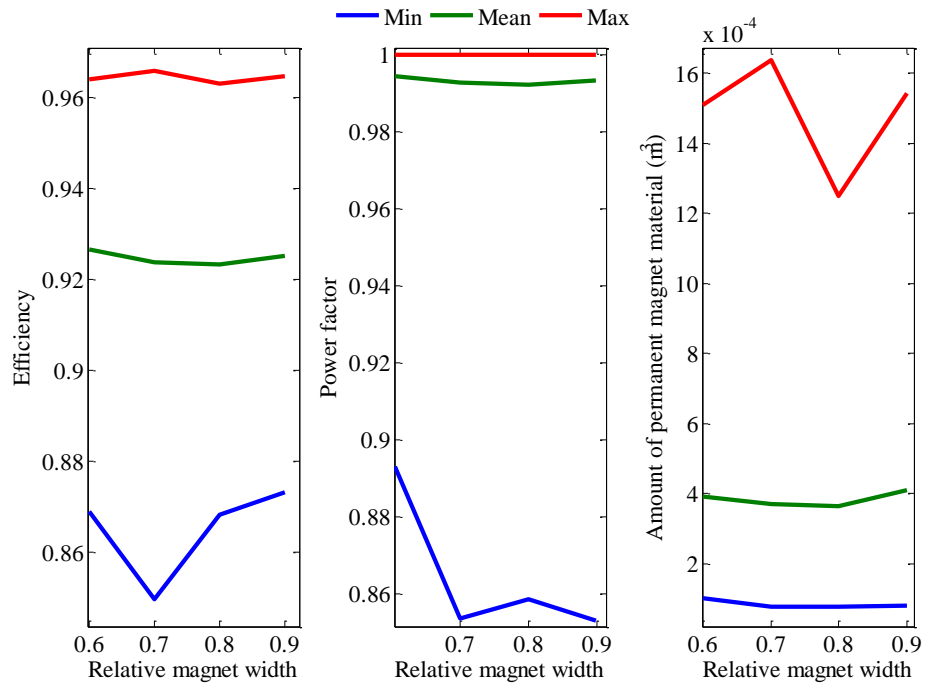


**Figure 23.** The machine properties as a function of the relative magnet width.

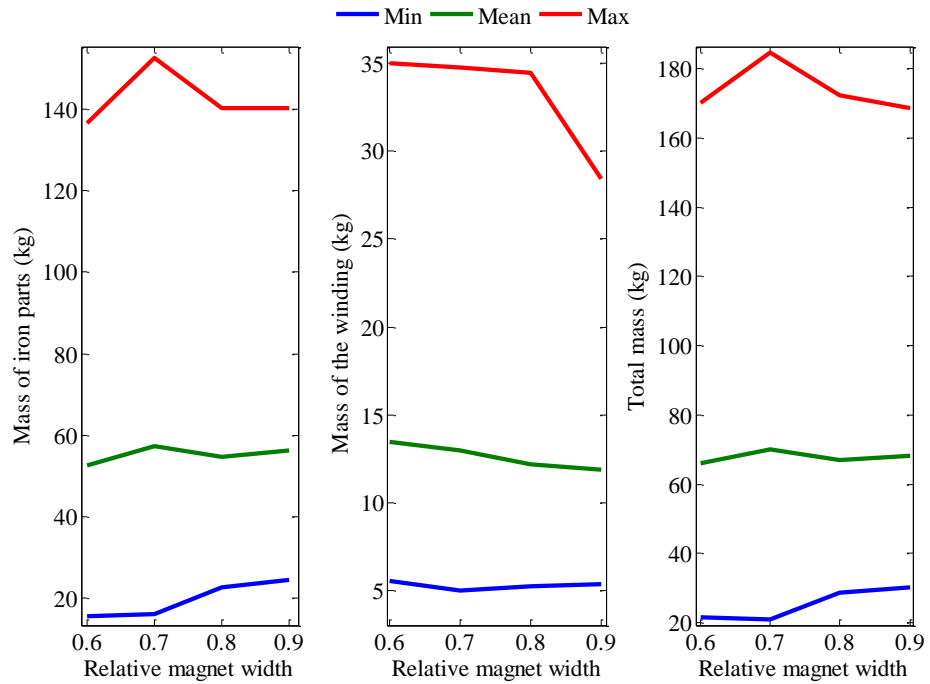


**Figure 24.** The effect of the relative magnet width on the mass of the machine.

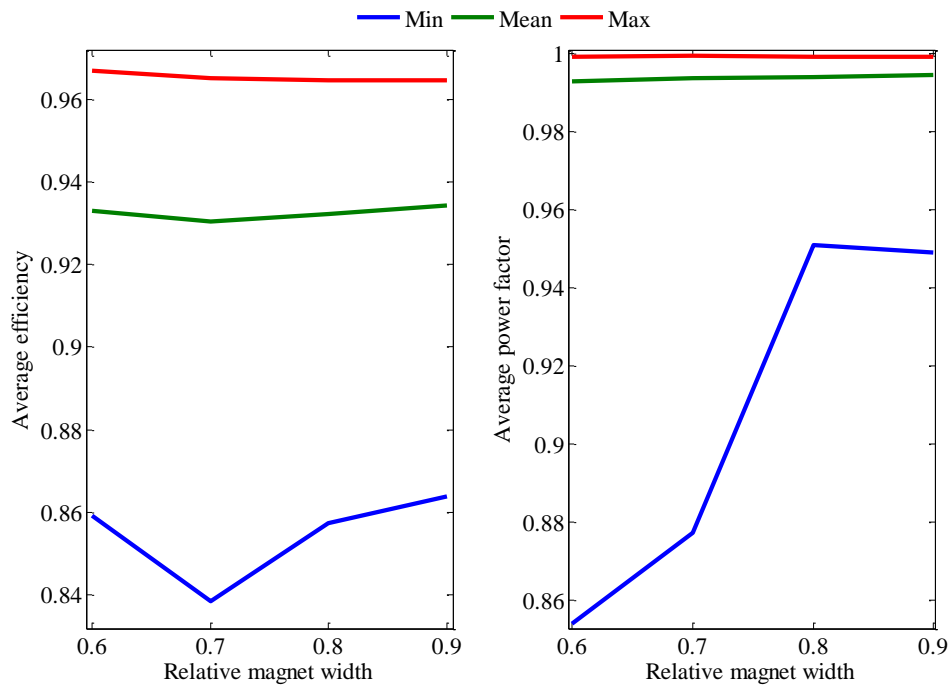


**Figure 25. The weighted averages of the efficiency and the power factor as a function of the relative magnet width.**

### 3.4.5 Current density

The effect of the initial value of stator winding current density is presented in Figure 26, Figure 27 and Figure 29. The initial value of the current density is a guess that is used to calculate the stator current. If a higher initial value is allowed, the current becomes higher which means that the losses should also be higher. Figure 28 shows how the obtained final current density depends on its initial value. The final value correlates quite well with the initial current density. It seems that the deviation is about  $\pm 0.5 \text{ A/mm}^2$  from the initial value.

The increase in the initial value of current density indeed decreases the efficiency. The maximum value obtained decreases from 0.966 to 0.948. Also the mass of the designs decreases when the current density increases. The effect is strongest on the mass of the windings but also the mass of the iron parts decreases as can be seen from Figure 27.

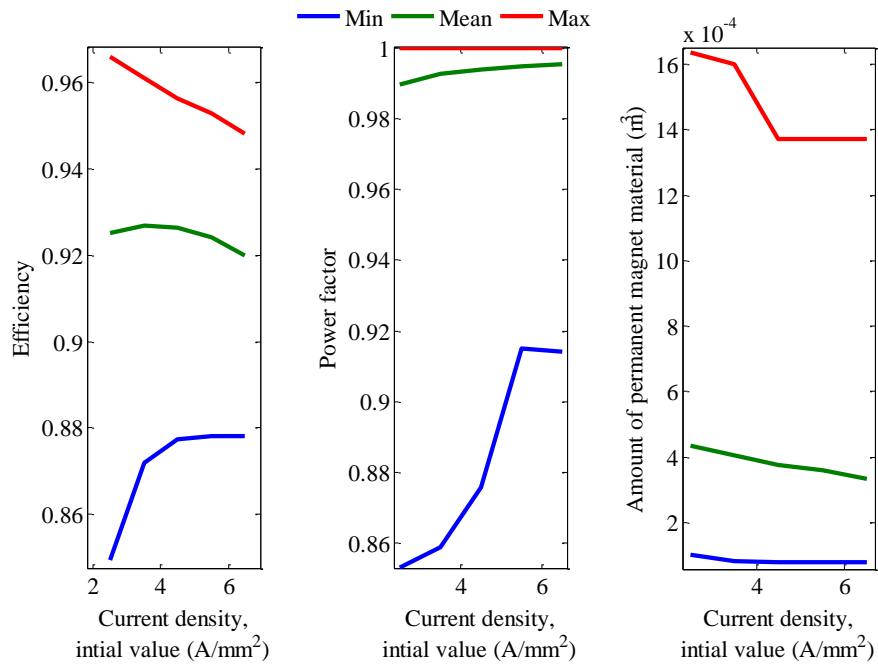


**Figure 26. The effect of the initial value of the current density in the stator.**

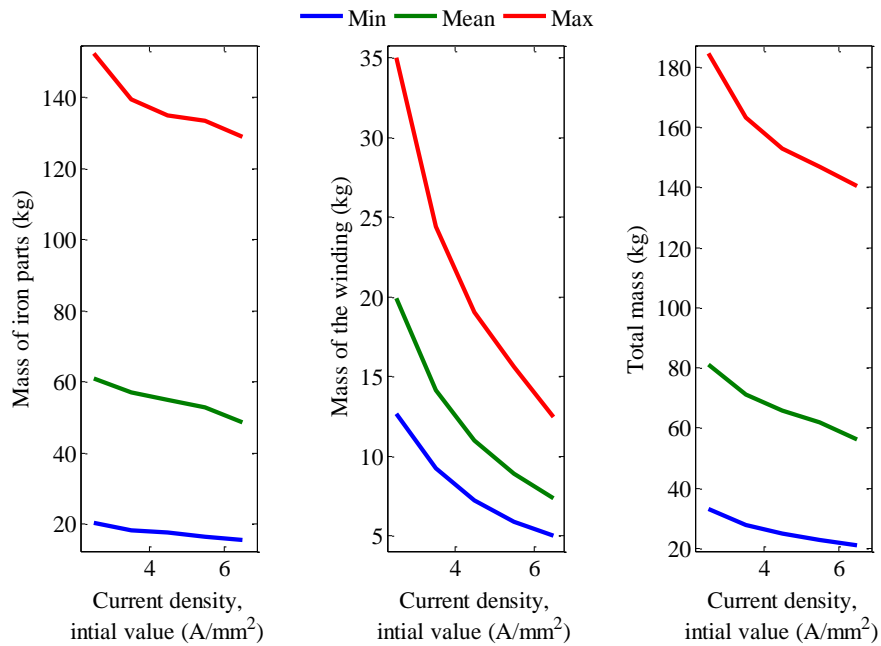


**Figure 27. The effect of the current density on the mass of the machine.**

The current density has an effect on the amount of permanent magnet material too. For example the minimum value was reduced from  $1.01 \cdot 10^{-3} \text{ m}^3$  to  $0.078 \cdot 10^{-3} \text{ m}^3$  when the current density was increased from  $2.5 \text{ A/mm}^2$  to  $6.5 \text{ A/mm}^2$ .

The maximum power factor is always one, but the mean value increases when the current density increases. However, the average power factor decreases even if the nominal one increases. The average efficiency is rather close to the nominal one.

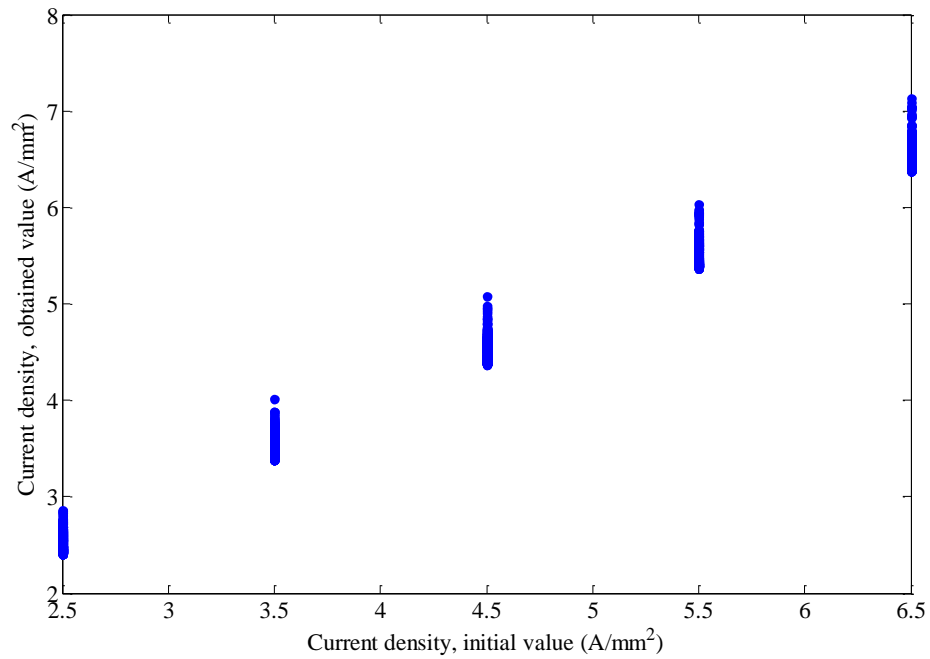


**Figure 28.** The dependency of the stator current density on the given initial value.

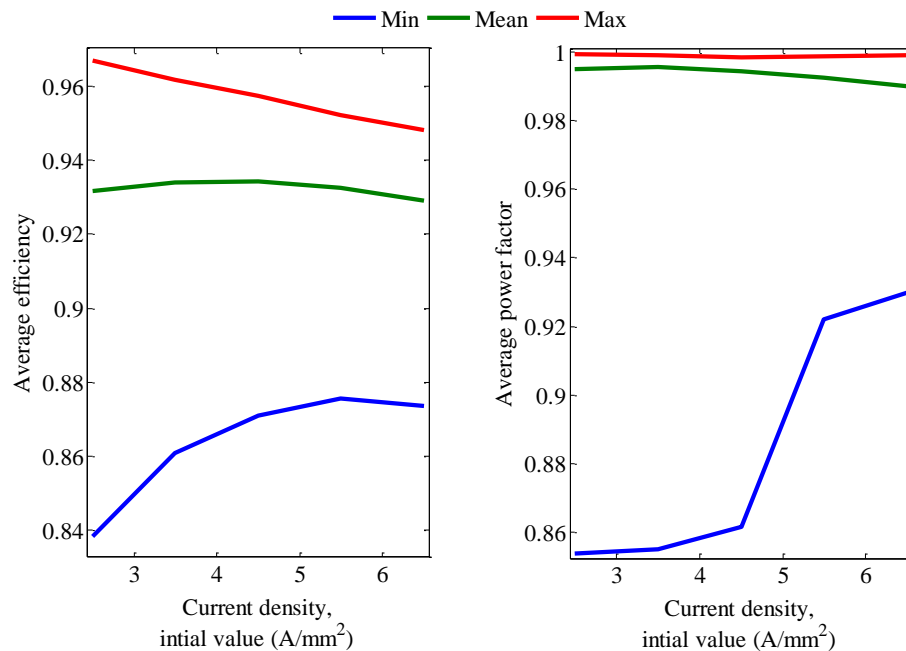


**Figure 29.** Average efficiency and power factor as a function of the initial value for current density.

### 3.4.6 Air gap flux density

The initial value of the air gap flux density affects also the flux densities in the stator yoke and teeth. As was explained earlier, the choice of the other flux densities is based on the initial value of the air-gap flux density. Also the desired linear current density in the stator is calculated using the initial guess for the air gap flux density. By allowing larger magnetic flux density in the machine, the machine size can be reduced. However, sometimes there is a quite large difference between the initial value of the air gap flux density and the realised one as can be seen from Figure 31. This is because the realised air gap flux density is calculated iteratively as shown in Figure 7.

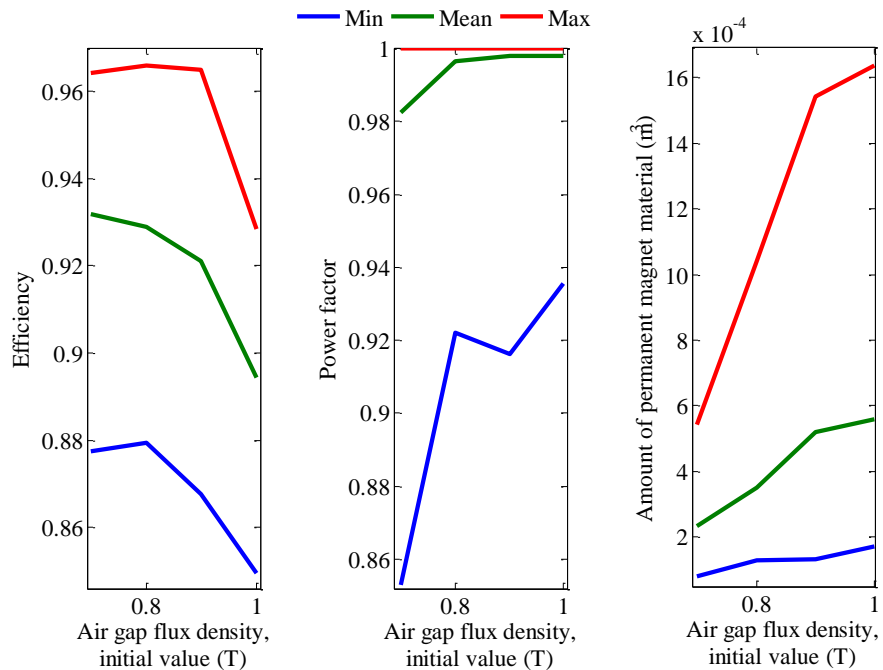


**Figure 30. The effect of the choice for the initial value of magnetic flux density in the air gap.**

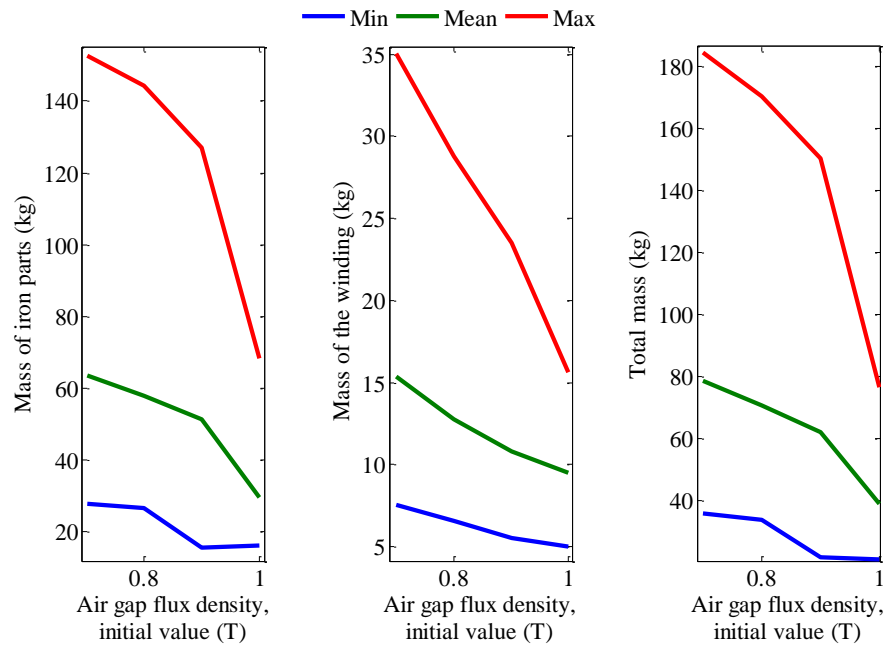


**Figure 31. The effect of the initial value of air gap flux density on the mass of the machine.**

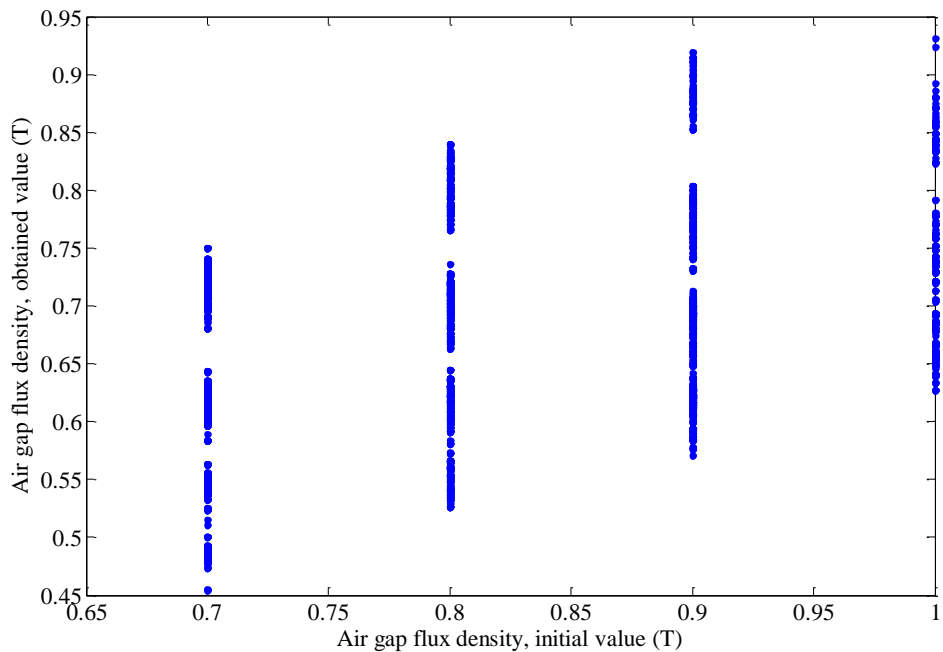


**Figure 32. Air gap flux density initial and final values.**

It can be seen from Figure 31 that by choosing a larger initial value for the magnetic flux density in the air gap, the mass of the machine can be reduced. This applies to both the mass of the iron parts and the mass of the winding. For example when the initial value of the air gap flux is 0.7 T, the minimum obtained mass is 36 kg

whereas with air gap flux initial value 1.0 T the minimum obtained mass was 21 kg. This is probably because the initial value of the magnetic flux density defines also the magnetic flux densities in the stator yoke and teeth. By allowing a larger flux density in the stator, the yoke and teeth become smaller, and the mass is thus reduced.

However, Figure 30 shows that the obtained efficiency becomes smaller with larger air gap flux density initial value. The power factor is better with higher initial values, but the maximum value is still one. The amount of magnet material needed increases when the magnetic flux value is increased. This is quite natural since the main flux is produced by the permanent magnets. Like the nominal efficiency, the average efficiency is also worse with larger air gap flux density values. The average power factor behaves in a slightly different way though. The maximum value is one, but there is quite much variation in the minimum value. The average value on the other hand does not change very much which means that the variations in the minimum values are probably caused by single solutions that can be considered as outliers with respect to the average power factor.

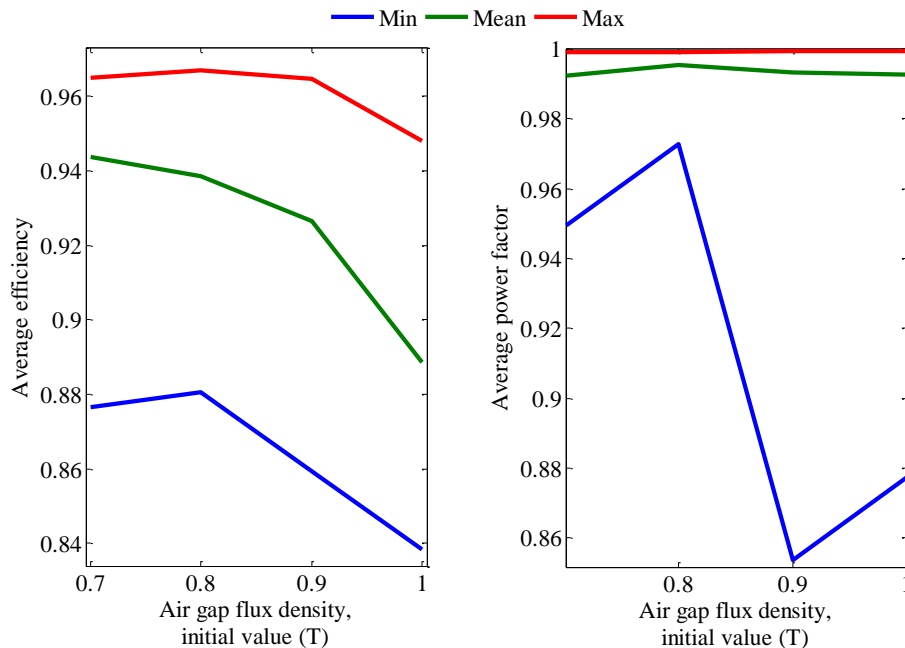


**Figure 33. The effect of air gap flux density initial value on the average efficiency and power factor.**

## 4 Discussion

### 4.1 Conclusions

The results are combined in Table 8. The table shows what happens to the investigated machine properties when the values of the different initial parameters are increased. In most cases, the results agreed well with the FEM calculations. However, there are still some differences in for example iron losses that have to be investigated.

**Table 8. Effect of initial parameters, 22 kW machine**

<b>Increasing parameter</b>	<b>Efficiency</b>	<b>Power factor</b>	<b>Machine size</b>	<b>Amount of permanent magnet material</b>
<b>Pole pair number</b>	decreases	maximum 1	decreases	decreases
$\chi$	increases	maximum 1	increases	increases
<b>Air gap</b>	slightly increases	maximum value 1	slightly decreases	slightly decreases
<b>Relative magnet width</b>	no clear effect	maximum 1	slightly increases	no clear effect
<b>Current density, initial value</b>	decreases	maximum 1, increases	decreases	slightly decreases
<b>Air gap flux density, initial value</b>	decreases	maximum 1, increases	decreases	increases

The effect of a change in the efficiency can be evaluated by calculating the energy costs during a certain time interval, for example 10 years. According to [17] the energy price for small industry is 4.34 c/kWh. The average power of the machine can be calculated from the operation profile presented in Section 2.3. For a 22 kW machine Equation (51) gives 8.39 kW for the average shaft power. If the efficiency decreases for example from 0.94 to 0.93 the difference in the energy costs becomes 365 € in 10 years. If the decrease in the efficiency is 0.1, the energy costs increase 4500 €.

For the material costs, one estimate for NdFeB-magnet material is 62 €/kg [2]. If the total volume of the magnets decreases 200 cm<sup>3</sup>, it means a 1.46 kg decrease in the mass and a 90.52 € decrease in the material costs. The conclusion is that if the machine is intended for long time use, the energy costs are larger and thus in this case it is more important to obtain good efficiency than to reduce the magnet volume.

Since the flux density in the stator yoke and teeth depends of the air gap flux density, changing the latter one will affect also to the two other values. Therefore the air gap flux density initial value can affect to the machine size. By increasing the air gap flux initial value, it is possible to decrease the machine size. However, this leads to decreased efficiency and increased amount of permanent magnet material.

This is reasonable, since the main flux is produced by the permanent magnets. The machine size decreases since larger flux density is allowed in the stator. However, the magnetic flux density cannot be made as large as possible, because when the flux density becomes larger than a certain value, the iron starts to saturate. After that, the flux density cannot be increased very much. According to the results, the optimal value for the air gap flux density is a compromise between the machine size and the amount of permanent magnet material used and efficiency.

The machine size can be decreased by increasing the current density. Also the amount of permanent magnet material will decrease slightly. When larger current density is allowed, it means that the conductors in the stator winding can be made smaller. The thinner conductors need smaller area in the stator slots, which means that the stator slots can be made smaller. This will also reduce the outer diameter of the stator core and therefore also the mass of the iron parts. The major drawback is that the efficiency decreases, presumably due to increased current losses. The power factor is improved slightly, although unity power factor is possible with smaller current densities as well.

The relative magnet width does not have very strong effect on any of the properties. By decreasing the magnet width, it is possible to slightly decrease the mass of the machine, but the effect is not very strong. The upper limit for the magnet width is the pole pitch.

Increasing the air gap slightly increases the efficiency and decreases the machine size, but the amount of permanent magnet material needed becomes larger. This happens because when the air-gap is made larger, the distance between the magnets and the stator winding increases, which means that thicker magnets are needed to produce enough flux to cause the machine to rotate. However, it was noticed that if the air gap was very small and the magnets were very thin, the eddy current losses in the magnets became huge. The optimal size of the air gap is thus a compromise between the machine size and the amount of permanent magnet material used. Its effect on the power factor is not significant since unity power factor is possible to achieve with any air gap size tested.

According to Table 8, if the  $\chi$  increases, the amount of magnet material decreases. The machine size seems to have minimum with  $\chi$  somewhere in the middle. The effect on the machine size is however indirect, and cannot be seen from these results, since the machine constant is not varied here. With larger stator inner diameter, more

slots will fit in. This means that it is possible to obtain a linear current density that corresponds to a larger machine constant and thus smaller machine.

Increasing the  $\chi$  causes the efficiency and power factor to decrease. This means basically that a shorter machine with larger diameter gives better efficiency and power factor. Also the machine size can be reduced by increasing the machine constant. The drawback of the larger value of  $\chi$  is that more magnet material is needed.

The number of poles affects strongly the size of the machine. With larger number of poles the machine becomes smaller, but if the rotation speed is kept constant, higher supply frequency is needed. For this reason the efficiency becomes worse with larger pole pair number since the losses depend of the frequency. By choosing the other parameters well, it is however possible to obtain a larger efficiency with larger number of poles. The amount of permanent magnet material is smaller when there are more poles.

The clearest results are the following:

- Increasing the number of poles will decrease both machine size and efficiency
- Increasing the machine length to air gap diameter ratio will increase the machine size and the amount of magnet material needed
- Larger initial value for the stator current density will decrease the machine size and efficiency
- Increasing the initial value of the air gap flux density will increase the amount of permanent magnet material needed
- The relative magnet width does not seem to have very strong effect on anything
- Choosing a smaller air-gap decreases the thickness of the permanent magnets
- Increasing the machine length to air gap ratio increases the efficiency

The purpose of this study was to find contradictive design parameters that could be used for optimization of a surface mounted permanent magnet synchronous machine. There seems to be a contradiction between the efficiency and the machine size. The machine size can be reduced by at least two ways: by increasing the pole pair number or the stator current density. Both of these methods also increase the losses, which means that the efficiency becomes worse. Also increasing the machine length to air gap diameter ratio  $\chi$  slightly improves the efficiency, but this means also increased machine size and amount of permanent magnet material. The power factor of a PMSM seems to be usually quite good which is also said in the literature.

## 4.2 Further work

With the dimensioning tool, it is possible to design a surface mounted permanent magnet synchronous machine. The design results can be modified to meet different requirements for different applications. It is easy to test how the results can be modified by changing different parameters. It is also possible to calculate the basic dimensioning for given initial conditions. It is rather easy to obtain a number of possible design solutions for a given design situation by changing the free parameters. The results can be used to analyse the design choices.

However, there are still some improvements that could be done. It is still somewhat difficult to present the results illustratively. This is partly because the amount of data is rather large, and partly because there are many varying parameters. One problem is that all possible combinations of the initial parameters do not give a reasonable design result. For example the obtained shaft power might become considerably smaller than the desired one. This is often due to high losses.

This means that it is not possible to use all possible combinations in the analysis, and during the results calculation process, also a lot of non-working solutions are generated. These have to be filtered out before starting to analyse. It also makes it more difficult to analyse the results. Because all the solutions are not optimal, the data points in the figures do not form a clear line or curve. If some kind of optimization algorithm would have been used, result data points would have formed some kind of optimal curve.

It has to be also remembered that the machine design process has multiple properties that have to be optimized. This means that the best solutions are always compromises between different criteria. From the optimization point of view, it could be useful, if some of the parameters could be combined somehow. One possibility could be to investigate if the efficiency and power factor could be combined. The optimal solution also depends on the application the machine is intended for. Sometimes for example the machine price might not have a great importance whereas the size could be critical. On some other cases however, the costs should be reduced as much as possible, which could reduce the use of the magnet material for instance.

In the example case of the 22 kW industrial pump, presumably the efficiency would be important because the pump is working 70 % of the working period. If the efficiency is poor, it means that losses are high which means that more energy is wasted and the energy costs of the pump become higher. Because the pump is designed for industrial use, it is presumably meant to last a rather long time. This means that the production and material costs are less important than the operating costs.

The conclusion is that to further improve the dimensioning tool, an optimization algorithm should be used. This would help finding the good combinations of initial parameters. However, without the optimization, it is possible to investigate also the worse results and see what kind of initial parameter combinations result to these.

At the moment, the dimensioning tool supports only surface mounted machines with single layer winding. These constructions were chosen for simplicity. With rather simple modifications, it would be possible to get the tool work also with double layer windings. This would make it also possible to compare different winding types with each other.

## References

1. Morimoto, S. Trends of Permanent Magnet Synchronous Machines. Transactions on Electrical and Electronic Engineering 2007, Vol. 2.
2. Gieras, J.F. & Wing, M. Permanent Magnet Motor Technology - Design and Applications. Marcel Dekker, Inc, 2002.
3. Current Primary and Scrap Metal Prices, Available: <http://www.metalprices.com/#>, Accessed 04.05.2012.
4. MathWorks/MATLAB Web Page, Available: [www.mathworks.com/products/matlab/](http://www.mathworks.com/products/matlab/), Accessed 03.05.2012.
5. Puranen, J. Induction Motor Versus Permanent Magnet Synchronous Motor in Motion Control Applications: a Comparative Study, Doctoral Thesis, Lappeenranta University of Technology, Acta Universitatis Lappeenrantaensis 249, 2006.
6. Guru, B.S. & Hiziroğlu, H.R. Electric Machinery and Transformers. 3rd ed. Oxford University Press, 2001. 726.
7. Heikkilä, T. Permanent Magnet Synchronous Motor for Industrial Inverter Applications - Analysis and Design. Dissertation, Lappeenranta University of Technology, Acta Universitatis Lappeenrantaensis 134, 2002.
8. Pyrhönen, J., Jokinen, T. & Hrabovcová, V. Design of Rotating Electrical Machines. John Wiley & Sons, Ltd., 2008.
9. Jussila, H. Napakäämityn murtovakokestomagneettitahtikoneen suunnittelu. Master's Thesis, Lappeenranta University of Technology, 2005.
10. Demetriades, G.D., Zelaya de la Parra, H., Andersson, E. & Olsson, H. A Real-Time Thermal Model of a Permanent Magnet Synchronous Motor. IEEE Transactions on Power Electronics 2010, Vol. 25, No. 2
11. Hafner, M., Schöning, M. & Hameyer, K. Automated sizing of permanent magnet synchronous machines with respect to electromagnetic and thermal aspects. COMPEL: The International Journal for Computation and Mathematics in Electrical and Electronic Engineering 2010, Vol. 25, No. 9.
12. Lindström, J., Thermal Model of a Permanent-Magnet Motor for a Hybrid Electric Vehicle. Department of Electric Power Engineering, Chalmers University of Technology, Göteborg, Sweden, 1999. Report No. 11R, ISSN: 1401-6176.

13. El-Refaie, A.M., Harris, N.C., Jahns, T.M. & Rahman, K.M. Thermal analysis of multibarrier interior PM synchronous Machine using lumped parameter model. IEEE Transactions on Energy Conversion 2004, Vol. 19, No. 2.
14. Kylander, G. Thermal modelling of small cage induction motors. Doctoral Thesis, Chalmers University of Technology, Göteborg, Sweden, 1995.
15. CEDRAT homepage, Available: [www.cedrat.com](http://www.cedrat.com), Accessed 09.05.2012.
16. Keränen, J.S. Calculation of validation data for permanent magnet machine dimensioning tool. Extended Abstract, TK3047 Electrical Product Concepts Team Workshop, Espoo: 2012.
17. Web Page of Energiemarkkinavirasto, Available: [www.energiemarkkinavirasto.fi](http://www.energiemarkkinavirasto.fi), Accessed 11.05.2012.
18. Piippo, A., Hinkkanen, M. & Luomi, J. Sensorless Control of PMSM Drives Using a Combination of Voltage Model and HF Signal Injection. Conference Record of the 39th IEEE-Industry Applications Society (IAS) Annual Meeting. Vol. 2. 2004.
19. Pillay, P. & Krishnan, R. Modeling of Permanent Magnet Motor Drives. IEEE Transactions on Industrial Electronics 1988, Vol. 34, No. 4.

## Appendix 1: Explanation of the d- and q-axis and the inductances

The synchronous machine is often presented using a two-axis model where the direct axis (d-axis) is in the direction of the pole and quadrature axis (q-axis) between the two poles. The equivalent circuit for a synchronous machine can be presented for d- and q-axis separately. The voltage equations for the d- and q-axis can be written as [18]

$$u_d = R_s i_d + \frac{d\psi_d}{dt} - \omega\psi_q \quad (\text{A1})$$

$$u_q = R_s i_q + \frac{d\psi_q}{dt} + \omega\psi_d \quad (\text{A2})$$

and the flux equations as

$$\psi_d = L_d i_d + \psi_{PM} \quad (\text{A3})$$

$$\psi_q = L_q i_q, \quad (\text{A4})$$

where  $u_d$  and  $u_q$  are the d- and q- components of the stator voltage,  $i_d$  and  $i_q$  are the d- and q-components of the stator current,  $\psi_d$  and  $\psi_q$  the components of the flux linkage and  $\psi_{PM}$  is the flux produced by the permanent magnets.  $R_s$  is the stator resistance and  $L_d$  and  $L_q$  are the d- and q-axis inductances.

An equivalent circuit model is presented in Figure 1. [19]

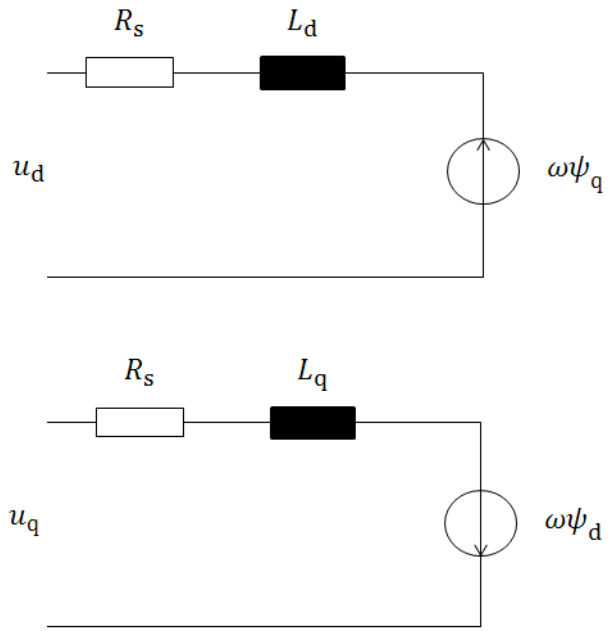


**Figure 1. Equivalent circuit of a PMSM in d- and q-axis.**

The inductances of the d- and q-axis consist of the magnetizing inductances  $L_{md}$ ,  $L_{mq}$  and the leakage inductance  $L_\sigma$ . The inductances at steady state are presented in

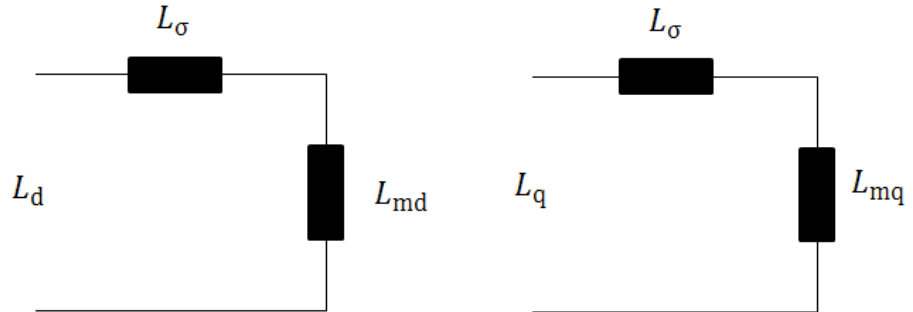


Figure 2.

**Figure 2. Inductances in the d- and q-axis at steady state.**

## Appendix 2: Dimensions and other parameters for validated models

Three models were validated. The shaft power was set to 22 kW, rotation speed to 1500 rpm, and phase voltage to 230 V for all three designs. The first design had 2 poles, the second one 8 poles and the third one 14 poles. The dimensions given by the dimensioning tool are given below for the three models.

### Dimensions for a 2-pole design

FINAL DESIGN

PHASE VOLTAGE (V)	230.94
NOMINAL SPEED (rpm)	1500.00
MACHINE CONSTANT (Ws/m <sup>3</sup> )	111185.00
Number of poles (-)	2
Supply frequency (Hz)	25.00
Effective length (mm)	318.1119
Actual length (mm)	313.1119
Actual air gap (mm)	2.5000
Stator outer diameter (mm)	308.8143
Stator inner diameter (mm)	159.0560
Number of slots (-)	48
Stator yoke height (mm)	50.7160
Filling factor for iron (-)	0.9500
Dimensions of the stator slots	
H1 (mm)	24.1632
H11 (mm)	1.0000
H13 (mm)	18.2566
B11 (mm)	4.0675
B12 (mm)	5.4233
B13 (mm)	7.8131
Rotor outer diameter (mm)	143.5560
Permanent magnet width (mm)	169.3934
Permanent magnet thickness (mm)	5.2500
Number of phases (-)	3
Number of parallel paths (-)	1
Conductors in a slot (-)	8
Conductor area (cross sect.) (mm <sup>2</sup> )	13.8874
Slot filling factor (-)	0.6000
Stator current (A)	35.9254

Shaft power at nominal speed (W)	22072.46
Torque at nominal speed (Nm)	140.52
Rotational speed (1/min)	1500.00
Air-gap flux density (T)	0.6297
Air-gap flux (Wb)	0.0339
eta at nominal speed (-)	0.9474
cos(phi) at nominal speed (-)	0.9361
Current density (A/mm <sup>2</sup> )	2.5869
Losses	
St. winding resistive (W)	489.63
Iron (W)	174.93
Additional (W)	167.78
Windage and ventilation (W)	81.83
Total (W)	1226.42
Stator resistance (ohm)	0.1265
D-axis inductance (H)	0.0306
Q-axis inductance (H)	0.0306
Temperatures	
Frame	40.0423
Yoke	42.2870
Teeth	44.6464
Winding	51.8297
Endwinding	75.8694
Magnets	59.6648
Bearings	41.8995

## Dimensions for the 8-pole design

### FINAL DESIGN

PHASE VOLTAGE (V)	230.94
NOMINAL SPEED (rpm)	1500.00
MACHINE CONSTANT (Ws/m <sup>3</sup> )	129268.13
Number of poles (-)	8
Supply frequency (Hz)	100.00
Effective length (mm)	164.2372
Actual length (mm)	159.2372
Actual air gap (mm)	2.5000
Stator outer diameter (mm)	287.7903
Stator inner diameter (mm)	205.2965
Number of slots (-)	48
Stator yoke height (mm)	14.3708
Filling factor for iron (-)	0.9500

Dimensions of the stator slots	
H1 (mm)	26.8762
H11 (mm)	1.0000
H13 (mm)	20.4807
B11 (mm)	4.5825
B12 (mm)	6.1099
B13 (mm)	8.7909
Rotor outer diameter (mm)	184.3365
Permanent magnet width (mm)	47.1937
Permanent magnet thickness (mm)	7.9800
Number of phases (-)	3
Number of parallel paths (-)	1
Conductors in a slot (-)	11
Conductor area (cross sect.) (mm <sup>2</sup> )	13.8874
Slot filling factor (-)	0.6000
Stator current (A)	37.9513
Shaft power at nominal speed (W)	22183.45
Torque at nominal speed (Nm)	141.22
Rotational speed (1/min)	1500.00
Air-gap flux density (T)	0.7084
Air-gap flux (Wb)	0.0055
eta at nominal speed (-)	0.9494
cos(phi) at nominal speed (-)	0.8886
Current density (A/mm <sup>2</sup> )	2.7328
Losses	
St. winding resistive (W)	378.85
Iron (W)	355.86
Additional (W)	167.78
Windage and ventilation (W)	78.31
Total (W)	1181.30
Stator resistance (ohm)	0.0877
D-axis inductance (H)	0.0025
Q-axis inductance (H)	0.0025
Temperatures	
Frame	40.2370
Yoke	41.6610
Teeth	44.3529
Winding	55.3147
Endwinding	69.9706
Magnets	58.1568
Bearings	42.3544

## Dimensions for the 14-pole design

FINAL DESIGN

PHASE VOLTAGE (V)	230.94
NOMINAL SPEED (rpm)	1500.00
MACHINE CONSTANT (Ws/m <sup>3</sup> )	157935.00
Number of poles (-)	14
Supply frequency (Hz)	175.00
Effective length (mm)	112.3042
Actual length (mm)	107.3042
Actual air gap (mm)	2.5000
Stator outer diameter (mm)	289.0034
Stator inner diameter (mm)	224.6083
Number of slots (-)	84
Stator yoke height (mm)	15.7226
Filling factor for iron (-)	0.9500
Dimensions of the stator slots	
H1 (mm)	16.4750
H11 (mm)	1.0000
H13 (mm)	12.1918
B11 (mm)	2.7407
B12 (mm)	3.6543
B13 (mm)	4.5663
Rotor outer diameter (mm)	207.4083
Permanent magnet width (mm)	34.4960
Permanent magnet thickness (mm)	6.1000
Number of phases (-)	3
Number of parallel paths (-)	1
Conductors in a slot (-)	8
Conductor area (cross sect.)(mm <sup>2</sup> )	6.3125
Slot filling factor (-)	0.6000
Stator current (A)	34.5130
Shaft power at nominal speed (W)	22335.49
Torque at nominal speed (Nm)	142.19
Rotational speed (1/min)	1500.00
Air-gap flux density (T)	0.7075
Air-gap flux (Wb)	0.0027
eta at nominal speed (-)	0.9350
cos(phi) at nominal speed (-)	0.9990
Current density (A/mm <sup>2</sup> )	5.4674
Losses	
St. winding resistive (W)	619.07
Iron (W)	639.98
Additional (W)	167.78
Windage and ventilation (W)	74.43
Total (W)	1552.69
Stator resistance (ohm)	0.1732

D-axis inductance (H)	0.0016
Q-axis inductance (H)	0.0016

Temperatures

Frame	40.4734
Yoke	43.6688
Teeth	46.7270
Winding	72.4993
Endwinding	96.7940
Magnets	52.4083
Bearings	42.3090